

---

# Variational Gaussian Process Diffusion Processes

---

**Prakhar Verma**  
Aalto University  
Espoo, Finland  
prakhar.verma@aalto.fi

**Vincent Adam**  
University Pompeu Fabra  
Barcelona, Spain  
vincent.adam@upf.edu

**Arno Solin**  
Aalto University  
Espoo, Finland  
arno.solin@aalto.fi

## Abstract

Diffusion processes are a class of stochastic differential equations (SDEs) providing a rich family of expressive models that arise naturally in dynamic modelling tasks. Probabilistic inference and learning under generative models with latent processes endowed with a non-linear diffusion process prior are intractable problems. We build upon work within variational inference approximating the posterior process as a linear diffusion process, point out pathologies in the approach, and propose an alternative parameterization of the Gaussian variational process using a continuous exponential family description. This allows us to trade a slow inference algorithm with fixed-point iterations for a fast algorithm for convex optimization akin to natural gradient descent, which also provides a better objective for the learning of model parameters.

## 1 Introduction

Continuous-time stochastic differential equations (SDEs, *e.g.* [51, 45]) are a ubiquitous modelling tool in fields ranging from physics [59] and finance [18] to biology [25] and machine learning [63, 49, 19, 37]. SDEs offer a natural and flexible way to encode prior knowledge and capture the dynamic evolution of complex systems, where the stochasticity and nonlinearity of the underlying processes play a crucial role. In the particular setting where the drift of the SDE model is linear, the resulting process is a Gaussian process (GP, [47]), known as a general and powerful ML paradigm of its own. We focus on diffusion processes (DPs), which are a subset of SDEs with additional regularity conditions on the drift and diffusion functions (details in Ch. 2 [27]). DPs with non-linear drifts cover a wide range of processes with *multi-modal*, *skew*, and *fat-tailed* behaviour (Fig. 2 left).

The generality of DPs, however, comes at a high practical cost: exact inference and parameter learning in non-linear DP models are computationally challenging or even intractable due to the infeasibility of direct simulation. Therefore, developing efficient and accurate methods for approximating DP models is crucial for theoretical and practical reasons. In this paper, we are concerned with Bayesian inference and learning in generative models with latent temporal processes endowed with an Itô DP prior.

Particularly, given a DP prior  $p$  and observations  $\mathcal{D}$ , we are interested in approximating the non-Gaussian DP posterior  $p_{|\mathcal{D}}$  with a linear-Gaussian DP  $q$  (Fig. 1). The seminal work by Archambeau et al. [7] used the framework of variational inference [9] to derive an approximate inference algorithm, where the approximating variational family  $\mathcal{Q}$  consists of time-variant linear (affine) DPs (*i.e.*, Markovian GPs, App. B in [47]):

$$q : d\mathbf{x}_t = f_q(\mathbf{x}_t, t) dt + \mathbf{L} d\boldsymbol{\beta}_t, \quad \mathbf{x}_0 \sim q(\mathbf{x}_0), \quad \text{s.t.} \quad f_q(\mathbf{x}_t, t) = \mathbf{A}_t \mathbf{x} + \mathbf{b}_t. \quad (1)$$

They also introduced an objective for approximate inference (the variational evidence lower bound or ELBO) and a fixed-point iteration algorithm to optimize it. In this paper, we highlight shortcomings in

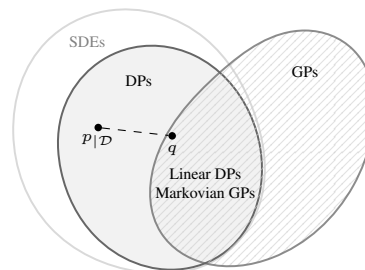


Figure 1: Approximating  $p_{|\mathcal{D}}$  with  $q$  for inference and learning in DPs.

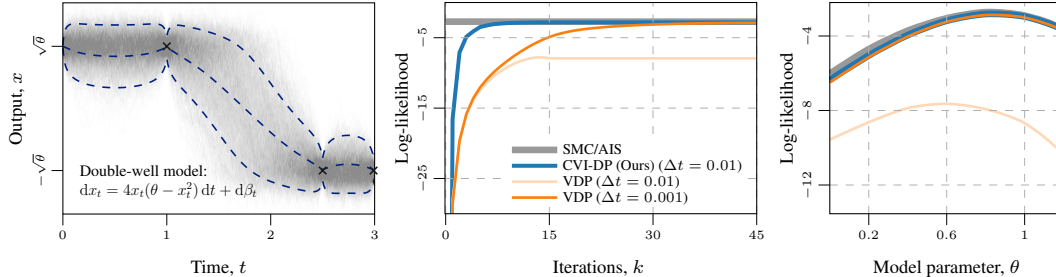


Figure 2: Left: Sequential Monte Carlo (SMC) samples along with the posterior of proposed method CVI-DP on a non-linear diffusion process with skew and two emerging modes in-between observations ( $\times$ ). Middle: ELBO iterations showcasing faster **inference** for the proposed method CVI-DP as compared to VDP. Right: The exact log-likelihood and ELBO as function of  $\theta$  for parameter **learning**.

the method proposed by Archambeau et al. [7], which we refer to as VDP: (i) the inference algorithm is slow to converge even in the simple setting of linear diffusions, and (ii) the parameterization of  $q$  via its drift function is ill-suited to the problem of learning the parameters of the prior diffusion from observations. To tackle these issues, we keep the same problem formulation and objective, but introduce an alternative parameterization [40, 15] of the variational process and a new optimization algorithm. Crucially, the new parameterization allows us to trade the slow fixed-point algorithm for a fast and better-understood algorithm for convex optimization, akin to natural gradient descent [4]. This stabilizes and drastically speeds up inference (Fig. 2 middle) and facilitates parameter learning.

The contributions of this paper are as follows: (i) We propose a novel site-based approach, the CVI-DP, for variational inference in diffusion processes that exploits the structure of the optimal variational posterior; (ii) We show how CVI-DP speeds up inference and learning under both linear and non-linear DP priors; and (iii) We demonstrate the feasibility and efficiency of our approach on a wide range of inference problems with DP priors featuring *multi-modal*, *skew*, and *fat-tailed* behaviours.

## 1.1 Related work

For inference in general non-linear Gaussian sequential models, particle filtering a.k.a. sequential Monte Carlo (SMC, *e.g.* [14]) methods are popular tools. When computing the posterior given some observations (the *smoothing* problem), conditional particle filters [5, 61, 39] have proven reliable in avoiding mode-collapse and particle degeneracy [55]. For the task of model parameter learning, advances in automatic differentiation have opened new possibilities for black-box learning of continuous-time dynamics (*e.g.*, [13, 48, 33]). Close to our work grounded in the framework of variational inference, Li et al. [37] introduced a tractable, sampling-based algorithm for inference and learning in general SDE models where the posterior process is parameterized via its non-linear drift and diffusion functions. However, although general in scope, these methods are unnecessarily heavy and compute-intensive for many practical applications. We take an alternative route, trading some generality—by restricting the posterior process to be a GP—for some efficiency. We do so by explicitly ‘Gaussianizing’ the non-Gaussian observations and linearizing the non-linear diffusion. These principles are well known *per se*, dating back to extended Kalman(–Bucy) filtering/smoothing (overview in Ch. 10 [51]) with numerous extensions (reviewed in [62]) such as posterior linearization [21, 22]. In ML, these methods have given rise to expectation propagation (EP, [41]) and variational inference (VI, [52, 9]).

This work aims at improving VDP originally proposed in [7, 8] (overview in Sec. 2.1). The algorithm has been used as a base for various other methods making it an important building block, *e.g.* in drift estimation [17] and switching systems [34], and learning neural network drift functions [50]. Our approach turns the hard problem of VI under a DP prior into an easier problem of VI under a GP prior. For the latter problem, it is common to restrict the variational process to a GP [11]. Efficient inference and learning algorithms that exploit the exponential family structure of the manifold of GPs and its geometry can then be derived which are now state of the art [31, 12, 2]. These algorithms are equivalent to natural gradient descent [4] and exploit the structure of the optimal variational process in the natural parameterization [52], splitting the contribution of the prior and the observations into the posterior in an additive fashion. These previous approaches consider models with GP priors and non-Gaussian likelihoods, while we focus on the more general problem of DP priors.

## 2 Variational inference and learning for diffusion processes

An Itô diffusion process (DP) with state dimension  $d$  can be defined by an SDE as

$$p : d\mathbf{x}_t = f_p(\mathbf{x}_t, t) dt + \mathbf{L} d\boldsymbol{\beta}_t, \quad \text{s.t. } \mathbf{x}_0 \sim p(\mathbf{x}_0), \quad (2)$$

where the drift  $f_p : \mathbb{R}^d \times \mathbb{R}_+ \rightarrow \mathbb{R}^d$  is a non-linear mapping, the diffusion term  $\mathbf{L}$  is linear (we drop dependency on  $t$  for notational convenience), and  $\boldsymbol{\beta}_t$  denotes the Brownian motion with a spectral density  $\mathbf{Q}_c$ . The data  $\mathcal{D} = \{(t_i, y_i)\}_{i=1}^n$  comprises input–output pairs and is assumed to constitute independent and identically distributed noisy versions of state trajectory  $\mathbf{x}$  at  $n$  ordered discrete-time points via an observation model providing the likelihoods  $\{p(y_i | \mathbf{x}_i = \mathbf{x}_t|_{t=t_i})\}_{i=1}^n$ . The posterior process  $p_{\mathbf{x}|\mathcal{D}}$  can be shown to have the following structural properties: (i) it shares the same diffusion coefficient as the prior; (ii) its can be expressed as the sum of the prior drift  $f_p$ , and a data and prior dependent term  $g$  resulting from a backward pass through the process and observations (see App. A):

$$p_{\mathbf{x}|\mathcal{D}} : d\mathbf{x}_t = f_p(\mathbf{x}_t, t) + g(\mathcal{D}, p, t) dt + \mathbf{L} d\boldsymbol{\beta}_t, \quad \text{s.t. } \mathbf{x}_0 \sim p_{\mathbf{x}|\mathcal{D}}(\mathbf{x}_0). \quad (3)$$

However, for most of the settings of interest, the posterior  $p_{\mathbf{x}|\mathcal{D}}$  is intractable and therefore approximate inference methods are used for both inference and learning.

Variational inference (VI) turns the inference problem into an optimization problem by introducing a variational distribution  $q$  over the latent variables  $\mathbf{x}$  and maximizing a lower bound  $\mathcal{L}(q)$  to the log marginal likelihood of the observations (or ELBO),

$$\log p(\mathbf{y}) \geq \mathbb{E}_q[\log p(\mathbf{y} | \mathbf{x})] - \text{D}_{\text{KL}}[q \| p] = \mathcal{L}(q), \quad (4)$$

where  $p$  is the prior distribution over  $\mathbf{x}$  and  $p(\mathbf{y} | \mathbf{x})$  is the likelihood derived from the observation model. The gap in the inequality can be shown to be  $\log p(\mathbf{y}) - \mathcal{L}(q) = \text{D}_{\text{KL}}[q \| p_{\mathbf{x}|\mathcal{D}}]$ . Thus, the bound is tight for  $q = p_{\mathbf{x}|\mathcal{D}}$ , *i.e.* when  $q$  is the posterior distribution. Note here that we use probability density functions to refer to the associated distributions, as is commonly done in the field.

In the case of diffusion processes, the KL divergence between the variational process  $q(\mathbf{x})$  and the prior process  $p(\mathbf{x})$  can be expressed by using Girsanov theorem [23] leading to the ELBO,

$$\mathcal{L}(q) = \mathbb{E}_{q(\mathbf{x})} \log p(\mathbf{y} | \mathbf{x}) - \frac{1}{2} \int_0^T \mathbb{E}_{q(\mathbf{x}_t)} \|f_q(\mathbf{x}_t, t) - f_p(\mathbf{x}_t, t)\|_{\mathbf{Q}_c^{-1}}^2 dt - \text{D}_{\text{KL}}[q(\mathbf{x}_0) \| p(\mathbf{x}_0)], \quad (5)$$

where  $\|\cdot\|_{\mathbf{Q}_c^{-1}}^2$  is the weighed 2-norm associated to the inner product  $\langle \mathbf{f}, \mathbf{g} \rangle_{\mathbf{Q}_c^{-1}} = \mathbf{f}^\top \mathbf{Q}_c^{-1} \mathbf{g}$ , and we set the diffusion function of the posterior process to its optimal value, which is that of the prior.

The prior DP might have free *model* parameters  $\boldsymbol{\theta}$  (*e.g.* parameterizing the drift function as in Fig. 2) that need to be adjusted to best explain the observations, a task we refer to as the learning problem. In this scenario, the ELBO  $\mathcal{L}(q, \boldsymbol{\theta})$  depends on both the model parameters  $\boldsymbol{\theta}$  and the variational distribution  $q$ . Noting  $q^*(\boldsymbol{\theta}) = \arg \max_q \mathcal{L}(q, \boldsymbol{\theta})$ , the optimal variational distribution for fixed model parameters  $\boldsymbol{\theta}$ , a common objective to solve the learning problem is to maximize objective  $\mathcal{L}(q^*(\boldsymbol{\theta}); \boldsymbol{\theta})$ . This nested optimization problem is intractable and usually replaced by coordinate ascent of the ELBO with respect to  $(q, \boldsymbol{\theta})$ , a procedure known as variational Expectation–Maximization (VEM, [43]). The efficacy of VEM strongly depends on the choice of parameterization for  $q$  and its dependence on  $q$  [2].

### 2.1 Gaussian variational inference for diffusion processes (VDP)

Archambeau et al. [7] propose to restrict the variational process  $q(\mathbf{x})$  to be a diffusion with affine drift

$$\mathcal{Q} = \{q : d\mathbf{x}_t = (\mathbf{A}_t \mathbf{x}_t + \mathbf{b}_t) dt + \mathbf{L} d\boldsymbol{\beta}_t, \quad \mathbf{x}_0 \sim q(\mathbf{x}_0)\}, \quad (6)$$

with  $\mathbf{A}_t \in \mathbb{R}^{d \times d}$  and  $\mathbf{b}_t \in \mathbb{R}^d$  corresponding to the set of Markovian Gaussian processes (*cf.*, Ch. 12 in [51]). In this setting, the marginal distribution  $q(\mathbf{x}_t)$  of the process are fully characterised by the mean and covariance  $\mathbf{M} = (\mathbf{m}_t, \mathbf{S}_t)$ . We summarize their method here, leaving details to App. C.

**Constrained optimization** Archambeau et al. express the ELBO Eq. (5) in terms of both the variational parameters  $\mathbf{V} = (\mathbf{A}_t, \mathbf{b}_t)$  via the drift function  $f_q$  and the marginal statistics  $\mathbf{M}$  via the expectations under  $q(\mathbf{x}_t)$ , which are coupled through ODEs:

$$C[\mathbf{M}, \mathbf{V}](t) = \begin{bmatrix} \dot{\mathbf{m}}_t - \mathbf{A}_t \mathbf{m}_t - \mathbf{b}_t \\ \dot{\mathbf{S}}_t - \mathbf{A}_t \mathbf{S}_t - \mathbf{S}_t \mathbf{A}_t^\top - \mathbf{Q}_c \end{bmatrix} = \mathbf{0} \quad \forall t. \quad (7)$$

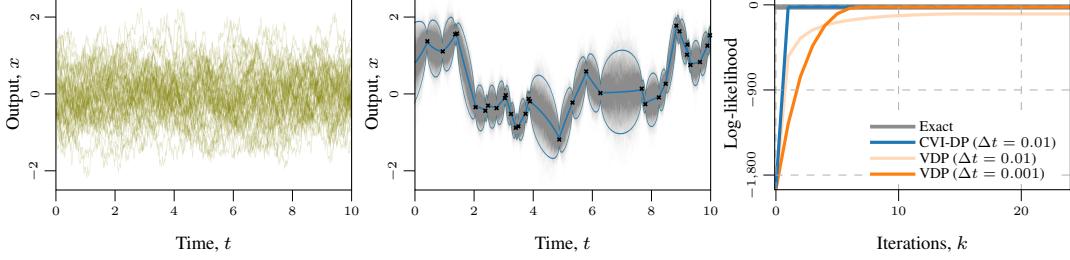


Figure 3: Approximate inference under a linear diffusion process (Ornstein–Uhlenbeck). Left: Draws from the prior. Middle: Approximate posterior process for CVI-DP overlaid over SMC ground-truth samples. Right: CVI-DP converges quickly even with large discretization step when inferring the variational parameters, while VDP suffers from slow convergence even with a small discretization step.

Therefore, optimization of the ELBO can be expressed as the optimization of

$$\mathcal{L}(\mathbf{M}, \mathbf{V}) = \mathbb{E}_{q(\mathbf{x})} \log p(\mathbf{y} | \mathbf{x}) - \frac{1}{2} \int_0^T \mathbb{E}_{q(\mathbf{x}_t)} \|\mathbf{A}_t \mathbf{x}_t + \mathbf{b}_t - f_p(\mathbf{x}_t, t)\|_{\mathbf{Q}_c^{-1}}^2 dt - \text{D}_{\text{KL}}[q(\mathbf{x}_0) \| p(\mathbf{x}_0)], \quad (8)$$

subject to constraint  $C[\mathbf{M}, \mathbf{V}](t) = \mathbf{0}, \forall t$ . They propose to solve this constrained optimization problem via the method of Lagrangian multipliers (see App. C). This approach does not lead to a closed-form expression for the solution, but gives stationarity conditions for the optimal variational parameters,

$$(\mathbf{A}_t^*, \mathbf{b}_t^*) = \Pi_{q^*(\mathbf{x}_t)}[f_p(\cdot, t)] + g(\mathcal{D}, \mathbf{A}^*, \mathbf{b}^*, t), \quad (9)$$

where  $\Pi_{q(\mathbf{x}_t)}[f_p(\cdot, t)]$  is the posterior linearization operator applied to the prior drift  $f_p(\cdot, t)$  defined by

$$\Pi_{q(\mathbf{x}_t)}[f_p(\cdot, t)] = \arg \min_{(\mathbf{A}_t, \mathbf{b}_t)} \mathbb{E}_{q(\mathbf{x}_t)} \left[ \|\mathbf{A}_t \mathbf{x}_t + \mathbf{b}_t - f_p(\mathbf{x}_t, t)\|_{\mathbf{Q}_c^{-1}}^2 \right]. \quad (10)$$

Informally, the operator finds the best linear approximation of the drift in a squared loss sense, in expectation over the posterior process.

**Fixed point iterative algorithm** These stationarity conditions imply an iterative algorithm,

$$(\mathbf{A}_t^{(k+1)}, \mathbf{b}_t^{(k+1)}) = \Pi_{q^{(k)}(\mathbf{x}_t)}[f_p(\cdot, t)] + g(\mathcal{D}, \mathbf{A}_t^{(k)}, \mathbf{b}_t^{(k)}, t). \quad (11)$$

for finding the variational parameters. An appealing property of these fixed point updates is that they mimic (up to the posterior linearization) the additive expression of the exact posterior drift in Eq. (3) (see App. C for details). As follow-up, Archambeau and Opper [6] made clear the connection to posterior linearization that is also used as an explicit sub-routine in approximation algorithms [20, 58].

**Limitations of the VDP method** The first issue is with the iterative algorithm in Eq. (11). The iterative algorithm is introduced out of convenience because it leads to closed-form updates. However, it does not come with convergence guarantees. Another issue stemming from the stationarity conditions Eq. (9) is that unlike in the exact inference case Eq. (3), the deviation  $g$  from the prior drift depends on the optimal posterior  $(\mathbf{A}^*, \mathbf{b}^*)$  instead of on the prior  $p$ . This dependence makes the fixed-point updates slow to converge—even for simple linear diffusion (see Fig. 3 right).

A downstream problem is in the learning of model parameters (via ELBO optimization) due to the parameterization choice of  $q$ . Following [2], we argue that when learning parameters via ELBO maximization, the best parameterization of the variational posterior  $q$  is one that completely decouples the contribution of the prior from that of the observations. It is not possible to achieve this when parameterizing  $q$  via its drift function. This is true even when exploiting the additive expression of the exact drift Eq. (3) because the deviation term  $g$  still mixes the prior and the observations. The algorithm proposed in [7] inherits this more general problem of parameterization via the drift function.

In the next section, we describe our method and how it fixes the aforementioned issues by exploiting the exponential family structure of linear diffusion processes. By parameterizing the posterior in terms of its natural parameters, (i) we bypass the need to use a fixed point algorithm, trading it for a well-understood convex optimization algorithm, and (ii) we achieve a better separation of the prior and observation contributions to the posterior, speeding up the dynamics of learning.

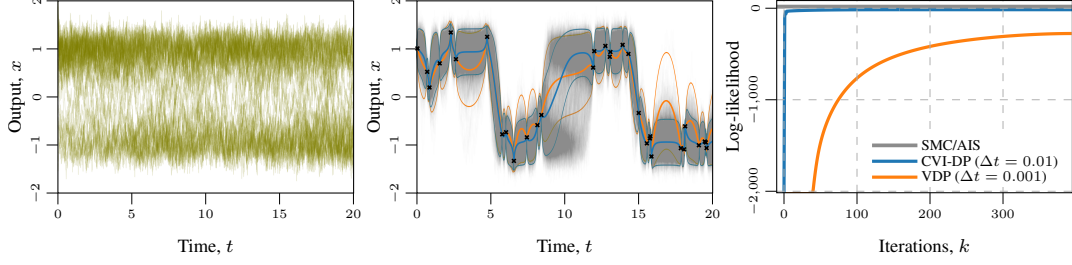


Figure 4: Approximate inference under a Double-Well prior (draws from prior on the left). Middle: Approximate posterior processes for CVI-DP and VDP overlaid on the SMC ground-truth samples. Right: CVI-DP converges quickly even with large discretization step when inferring the variational parameters, while VDP suffers from slow convergence even with a small discretization step.

### 3 Conjugate-variational inference for diffusion processes (CVI-DP)

We focus on performing approximate inference in non-linear diffusion process priors and an arbitrary likelihood. Our approach hinges on the following steps: (i) We frame our method within the framework of variational inference, restricting the variational process to the set of linear diffusions; (ii) such a variational process belongs to an exponential family, and we parameterize it via its natural parameters; (iii) we speed up inference via natural gradient descent and ease learning by incorporating iterative posterior linearization of the prior in the framework. In the following sections, we proceed step-by-step in deepening and devising this setup.

#### 3.1 Inference in models with linear diffusions and Gaussian observation model

Consider the following continuous-discrete Gaussian diffusion model with Gaussian observations:

$$d\mathbf{x}_t = (\mathbf{A}_t \mathbf{x}_t + \mathbf{b}_t) dt + \mathbf{L} d\beta_t \quad \text{and} \quad y_i | \mathbf{x} = \mathbf{h}^\top \mathbf{x}_{t_i} + \varepsilon_i, \quad (12)$$

with  $\varepsilon_i \sim \mathcal{N}(0, \sigma^2)$  and  $\mathbf{h} \in \mathbb{R}^d$  (example of such a model in Fig. 3). The diffusion process can be marginalized to state evaluations at data input  $\{\mathbf{x}_i = \mathbf{x}_{t_i}\}_{i=1}^N$  leading to the discrete-time Markov chain

$$\mathbf{x}_{i+1} = \hat{\mathbf{A}}_i \mathbf{x}_i + \hat{\mathbf{b}}_i + \hat{\varepsilon}_i, \quad \hat{\varepsilon}_i \sim \mathcal{N}(\mathbf{0}, \hat{\mathbf{Q}}_i), \quad (13)$$

where  $(\hat{\mathbf{A}}_i, \hat{\mathbf{b}}_i, \hat{\mathbf{Q}}_i)$  are available in closed-form. The state vector is distributed as a multivariate Gaussian, with Markovian structure, whose probability density function factorizes as  $p(\mathbf{x}_0, \dots, \mathbf{x}_N) = p(\mathbf{x}_0) \prod_{i=1}^N p(\mathbf{x}_i | \mathbf{x}_{i-1})$ . The marginalized process belongs to the exponential family  $\mathcal{F}$  which we define as containing non-degenerate multivariate Gaussians with a probability density

$$p(\mathbf{x}_0, \dots, \mathbf{x}_N) = \exp[\langle \mathbb{T}(\mathbf{x}), \boldsymbol{\eta}_p \rangle - A(\boldsymbol{\eta}_p)], \quad (14)$$

where  $\mathbb{T}(\mathbf{x}) = [\mathbf{x}, \text{btd}(\mathbf{x}\mathbf{x}^\top)]$  is the set of sufficient statistics with  $\text{btd}(\mathbf{M})$  sets entries of  $\mathbf{M}$  outside of the  $d$ -block tri-diagonals to zero (see App. D.1). The natural parameters of the prior  $\boldsymbol{\eta}_p$  are related to the prior mean  $\mathbf{m}_p$  and covariance  $\mathbf{S}_p$  of the distribution via  $\boldsymbol{\eta}_p = [\mathbf{S}_p^{-1} \mathbf{m}_p, -\frac{1}{2} \mathbf{S}_p^{-1}]$ . Each of the likelihood factors  $p(y_i | \mathbf{x}_i)$  can be expressed as proportional to the density of an exponential family distribution conjugate to  $\mathcal{F}$  with sufficient statistics  $\mathbb{T}(\mathbf{h}^\top \mathbf{x}_i)$  and natural parameters  $\boldsymbol{\lambda}_i^* = (\sigma^{-2} y_i, -\frac{1}{2} \sigma^{-2})$ , which we stack into the vector pair  $\boldsymbol{\lambda}^* = (\sigma^{-2} \mathbf{y}, -\frac{1}{2} \sigma^{-2}) \in \mathbb{R}^{N \times 2}$ . Thus, due to the conjugacy, the posterior distribution  $p(\mathbf{x} | \mathbf{y}) \propto p(\mathbf{y} | \mathbf{x}) p(\mathbf{x})$  belongs to  $\mathcal{F}$ . More formally, noting  $\mathbf{H} = \mathbf{I}_N \otimes \mathbf{h} \in \mathbb{R}^{N \times d}$  and introducing the linear projection  $\phi(\boldsymbol{\lambda}) = (\mathbf{H} \boldsymbol{\lambda}_1, \mathbf{H} \text{diag}(\boldsymbol{\lambda}_2) \mathbf{H}^\top)$ , the natural parameters of the posterior separate contribution of the prior and the observation in an additive manner,  $\boldsymbol{\eta}_{\mathcal{D}} = \boldsymbol{\eta}_p + \phi(\boldsymbol{\lambda}^*)$ . In this setting, the marginal likelihood also has a closed-form expression,  $p(\mathbf{y}) = \mathcal{N}(\mathbf{H} \mathbf{m}_p, \mathbf{H} \mathbf{S}_p \mathbf{H}^\top + \sigma^2 \mathbf{I}_n)$ , allowing gradient-based optimization of prior hyperparameters.

#### 3.2 Inference in models with linear diffusions and arbitrary observation model

When the observation model is not Gaussian, we can still marginalize the diffusion to a finite Markov chain. However, the posterior no longer belongs to an exponential family  $\mathcal{F}$ , and we need to resort to

approximate inference. Under the variational framework, restricting  $q$  to belong to  $\mathcal{F}$  has the convenient property that the optimal posterior has the same additive decomposition as in the conjugate case:  $\boldsymbol{\eta}_q^* = \boldsymbol{\eta}_p + \phi(\boldsymbol{\lambda}^*)$ , with  $\boldsymbol{\lambda}^* = (\boldsymbol{\lambda}_1^*, \boldsymbol{\lambda}_2^*)$ . This is revealed by looking at the first-order stationary condition of the optimal distribution  $q^*$ . Distributions in  $\mathcal{F}$  can be parameterized via their natural parameters  $\boldsymbol{\eta}$  but equivalently by their expectation parameters  $\boldsymbol{\mu} = \mathbb{E}[\mathbf{T}(\mathbf{x})]$ . The gradient of the ELBO with respect to the expectation parameters  $\boldsymbol{\mu}$  of  $q$  is given by  $\nabla_{\boldsymbol{\mu}} \mathcal{L} = \nabla_{\boldsymbol{\mu}} \mathbb{E}_q[\log p(\mathbf{y} | \mathbf{x})] - (\boldsymbol{\eta}_q - \boldsymbol{\eta}_p)$ , where we used the property  $\nabla_{\boldsymbol{\mu}} \text{D}_{\text{KL}}[q \| p] = \boldsymbol{\eta}_q - \boldsymbol{\eta}_p$ . At the optimum,

$$\nabla_{\boldsymbol{\mu}} \mathcal{L}|_{\boldsymbol{\mu}^*} = \mathbf{0} \implies \boldsymbol{\eta}_q^* = \boldsymbol{\eta}_p + \nabla_{\boldsymbol{\mu}} \mathbb{E}_q[\log p(\mathbf{y} | \mathbf{x})]|_{\boldsymbol{\mu}^*}. \quad (15)$$

The gradient of the expected log-likelihood can be shown to be sparse and low rank, *i.e.*  $\exists \boldsymbol{\lambda}^*, \phi(\boldsymbol{\lambda}^*) = \nabla_{\boldsymbol{\mu}} \mathbb{E}_q[\log p(\mathbf{y} | \mathbf{x})]|_{\boldsymbol{\mu}^*}$ . To find the optimal variational parameters, it is sufficient to search the space of distribution in  $\mathcal{F}$  with natural parameters  $\boldsymbol{\eta}_q = \boldsymbol{\eta}_p + \phi(\boldsymbol{\lambda})$ . Conjugate-computation VI (CVI, [31]) gives an efficient algorithm to find the optimal  $\boldsymbol{\lambda}^*$  by running mirror descent with the Kullback–Leibler divergence (KL) as Bregman divergence. More precisely, using  $\rho$  step-size, it constructs a sequence of iterates  $\boldsymbol{\lambda}^{(k)}$  via

$$\boldsymbol{\mu}^{(k+1)} = \arg \max_{\boldsymbol{\mu}} \langle \nabla_{\boldsymbol{\mu}} \mathcal{L}(\boldsymbol{\mu}^{(k)}), \boldsymbol{\mu} \rangle - \frac{1}{\rho} \text{D}_{\text{KL}}[q(\mathbf{x}; \boldsymbol{\mu}) \| q(\mathbf{x}; \boldsymbol{\mu}^{(k)})]. \quad (16)$$

This maximization can be computed in closed-form leading to updates in the natural parameterization

$$\boldsymbol{\lambda}^{(k+1)} = (1 - \rho) \boldsymbol{\lambda}^{(k)} + \rho \phi^{-1}(\nabla_{\boldsymbol{\mu}} \mathbb{E}_{q^{(k)}}[\log p(\mathbf{y} | \mathbf{x})]). \quad (17)$$

In the case of Gaussian observations, the gradient term in the updates is independent of where the gradient is evaluated and equal to  $\boldsymbol{\lambda}^*$ , so a *single step* of CVI with step-size  $\rho = 1$  leads to the optimum (see Fig. 3 for an empirical example). In the more general setting of log-concave likelihoods, the iterations in Eq. (17) are guaranteed to converge to the optimum.

### 3.3 Inference in non-linear diffusions with arbitrary observation model

Finally, we consider the challenging setting of non-linear diffusions. Similar to the algorithm proposed in [6], we adopt the variational approach and restrict the posterior process to the set of linear diffusions. However, instead of directly parameterizing the linear drift of the variational, we extend the finite Markovian exponential family to the continuous setting. Intuitively, such a continuous exponential family  $\mathcal{F}_c$  can be constructed as the infinite limit of small increments in the input space (the  $dt \rightarrow 0$  limit). More precisely, we introduce the sufficient statistics  $\mathbf{T}[\mathbf{x}] = [\mathbf{x}_t, \mathbf{x}_t(\mathbf{x}_t + d\mathbf{x}_t)^\top]_{t \in [0, T]}$ , and denote by  $\boldsymbol{\eta}(\cdot)$  and  $\boldsymbol{\mu}(\cdot)$  the associated natural and expectation parameters which are now functions indexed by time. Restricting the variational process to belong to  $\mathcal{F}_c$  means we force its drift to be linear. Our aim here is to parameterize the posterior so as to maintain, as much as possible, the additive separation of the contribution of the prior and observations to the natural parameterization of the posterior.

Unlike the case of linear diffusion, the Kullback–Leibler divergence in the ELBO and its gradient is no longer tractable. We side-step this problem by introducing a base distribution  $b \in \mathcal{F}_c$  that we will specify later to approximate the prior process  $p$ . With such a reference process  $b$ , we rewrite the ELBO as

$$\mathcal{L}(q) = \mathbb{E}_q[\log p(\mathbf{y} | \mathbf{x})] + \underbrace{(\text{D}_{\text{KL}}[q \| b] - \text{D}_{\text{KL}}[q \| p])}_{e(q,p,b)} - \text{D}_{\text{KL}}[q \| b]. \quad (18)$$

This corresponds to the ELBO of an alternative inference problem in a generative model with linear prior diffusion  $b$ , observations  $\mathcal{D}$ , and an additional implicit likelihood whose expected logarithm is given by  $e(q, p, b)$ . This term can be interpreted as an error quantifying how good  $b$  is in approximating  $p$  in the context of the variational distribution  $q$ . Crucially,  $e(q, p, b = p) = 0$  is only achievable when  $p$  is a linear diffusion. The first-order stationarity conditions for an optimum are

$$\boldsymbol{\eta}_q^* = \boldsymbol{\eta}_b + \underbrace{\nabla_{\boldsymbol{\mu}} \mathbb{E}_q[\log p(\mathbf{y} | \mathbf{x})]|_{\boldsymbol{\mu}^*}}_{\phi_c(\boldsymbol{\lambda}^*)} + \underbrace{\nabla_{\boldsymbol{\mu}} e(q[\boldsymbol{\mu}], p, b)|_{\boldsymbol{\mu}^*}}_{\boldsymbol{\Lambda}^*}, \quad (19)$$

---

**Algorithm 1:** Inference under a non-linear DP prior  $p(\mathbf{x})$  subject to observations

---

**Input:** Priors  $p(\mathbf{x})$ ,  $q(\mathbf{x})$ , data  $\mathcal{D}$ , learning rate  $\rho$

**while not converged do**

**while not converged do**

        Sites update:

$$\boldsymbol{\lambda}^{(k+1)} = (1 - \rho) \boldsymbol{\lambda}^{(k)} + \rho \phi_c^{-1}(\nabla_{\boldsymbol{\mu}} \mathbb{E}_q \log p(\mathbf{y} | \mathbf{x}))$$

$$\boldsymbol{\Lambda}^{(k+1)} = (1 - \rho) \boldsymbol{\Lambda}^{(k)} + \rho \nabla_{\boldsymbol{\mu}} e(q, p, b)$$

        Compute posterior:

$$\boldsymbol{\eta}_q^{(k+1)} = \boldsymbol{\eta}_b + \boldsymbol{\lambda}^{(k+1)} + \boldsymbol{\Lambda}^{(k+1)}$$

**end**

    Update  $b$ :  $b^{\text{new}} \leftarrow e(p(\mathbf{x}), q(\mathbf{x}))$

    Update  $\boldsymbol{\Lambda}$  under  $b^{\text{new}}$ :  $\boldsymbol{\Lambda}|_{b^{\text{new}}} = \boldsymbol{\Lambda}|_b + \boldsymbol{\eta}_b - \boldsymbol{\eta}_{b^{\text{new}}}$

**end**

---

Table 1: Negative log predictive density (NLPD) (lower better) over 5-fold CV for Gaussian (sanity check) and non-Gaussian DPs when performing **inference** only. CVI-DP agrees with the SMC ground-truth, even at large discretization steps  $\Delta t$  while VDP suffers from convergence issues.

		OU (Gaussian)	Beneš	DW	Sine	Sqrt
Baseline	SMC	0.371±0.225	0.178±0.160	0.069±0.140	0.153±0.210	-0.054±0.085
	Opt. Gaussian	0.374±0.234	0.172±0.167	0.077±0.117	0.160±0.215	-0.046±0.086
	GPR (OU kernel)	0.377±0.241	0.191±0.130	0.252±0.091	0.220±0.281	0.648±1.371
$\Delta t$ 0.01	VDP [7]	1.842±2.494	0.253±0.128	0.412±0.231	0.208±0.169	0.162±0.155
	CVI-DP (Ours)	0.377±0.239	0.169±0.153	0.076±0.186	0.154±0.207	-0.048±0.078
$\Delta t$ 0.005	VDP [7]	0.379±0.241	0.174±0.101	0.384±0.215	0.160±0.191	0.070±0.146
	CVI-DP (Ours)	0.377±0.240	0.169±0.153	0.075±0.190	0.154±0.207	-0.050±0.078
$\Delta t$ 0.001	VDP [7]	0.377±0.240	0.154±0.126	0.318±0.228	0.167±0.193	0.059±0.144
	CVI-DP (Ours)	0.377±0.241	0.169±0.153	0.075±0.192	0.154±0.208	-0.050±0.078

where  $\lambda^*$  is sparse in time and depends on the observations whereas  $\Lambda^*$  is dense and  $\phi_c(\lambda)(t) = (\sum_{i=1}^N \mathbf{h}\lambda_{i,1}\delta_{t=t_i}, \sum_{i=1}^N \mathbf{h}\mathbf{h}^\top \lambda_{i,2}\delta_{t=t_i})$ . By parameterizing the posterior as  $\eta_q = \eta_b + \phi_c(\lambda) + \Lambda$ , we can perform inference via the same mirror descent procedure as in Sec. 3.2 and get the iterative updates

$$\lambda^{(k+1)} = (1 - \rho)\lambda^{(k)} + \rho\phi_c^{-1}(\nabla_{\mu}\mathbb{E}_{q^{(k)}}[\log p(\mathbf{y} | \mathbf{x})]), \quad (20)$$

$$\Lambda^{(k+1)} = (1 - \rho)\Lambda^{(k)} + \rho\nabla_{\mu}e(q, p, b). \quad (21)$$

Details on the derivation of these updates are given in App. F.2. We are left to choose the base process  $b$ . For inference (optimizing for  $q$  given a fixed generative model) and under mild regularity conditions on the objective, it can be set arbitrarily: the iterative updates Eq. (20) and Eq. (21) can reach the optimal variational parameters irrespective of the base  $b$  and initial variational parameters  $\lambda^{(0)}, \Lambda^{(0)}$ . The simpler settings of prior diffusions with linear drifts and Gaussian observations shed some light on how to choose the base. Indeed, in the case of Gaussian observations,  $\lambda^*$  is independent of the prior  $p$  and captures all there is to know about the observations. To decouple the contributions of the prior and observations in the posterior, it is desirable to have  $\Lambda^*$  be independent of the observations. This is naturally achieved in the case of linear diffusion priors by setting the base to the prior ( $b = p$ ); in that case, we have  $e(q, p, b) = 0, \forall q$  and thus  $\Lambda^* = \mathbf{0}$ : we recover the efficient scheme of Sec. 3.2 for both inference and learning in models with linear diffusion priors.

Equipped with this insight, we return to the general setting of non-linear diffusions and propose to set  $b$  so as to minimize the proxy objective  $e(q^*, p, b)$ . An alternative expression for  $e$  reveals the connection of this approach to posterior linearization introduced in Eq. (10),

$$e(q, p, b) = \int \|f_b - f_p\|_{\mathbf{Q}_c^{-1}}^2 dq(x) + 2 \int \langle f_q - f_b, f_b - f_p \rangle_{\mathbf{Q}_c^{-1}} dq(x). \quad (22)$$

Indeed, posterior linearization minimizes the first term of Eq. (22). In this work, we choose to set  $b$  iteratively via posterior linearization within a broader algorithm for inference and learning, which we call CVI-DP and describe in Alg. 1. In CVI-DP, we alternate steps of (i) inference via mirror descent on  $\mathcal{L}(q, \theta)$  with respect to  $q$ , (ii) posterior linearization to update base  $b$ , and (iii) learning via gradient descent on  $\mathcal{L}(q(\theta), \theta)$  with respect to hyperparameters  $\theta$ .

**Comparison with the VDP method** CVI-DP is built on top of efficient algorithms specialized for the setting of linear diffusion priors (*i.e.*, GPs). One of its good properties is that it reverts to these efficient algorithms when applied to problems in the linear-Gaussian setting. In that sense, it unifies variational inference in models with a GP and a DP prior. This is unlike the VDP, which is very inefficient in these scenarios in terms of speed of convergence for both inference and learning (*cf.* Figs. 3 to 5). However, the parameterization of CVI-DP is slightly more costly than that of VDP. Both methods implicitly learn the transition statistics  $(\hat{\mathbf{A}}_i, \hat{\mathbf{b}}_i, \hat{\mathbf{Q}}_i)$  of a linear Gaussian state space model (see Eq. (13)), but VDP does not learn the  $\hat{\mathbf{Q}}_i$  and restricts the diffusion coefficient to match that of the prior diffusion. This is suboptimal when the continuous algorithm is discretized at implementation time: in Fig. 4 we show that the performance of VDP degrades fast as the discretization gets coarser, while the performance of CVI-DP is relatively unaffected.

Table 2: Negative log predictive density (NLPD) (lower better) over 5-fold CV for Gaussian (sanity check) and non-Gaussian DPs when performing **inference and learning**. CVI-DP yields good performance even at large discretization steps  $\Delta t$  while VDP suffers from convergence issues.

	OU (Gaussian)	Beneš	DW	Sine	Sqrt
GPR (OU kernel)	0.389±0.249	0.197±0.164	0.218±0.091	0.214±0.202	0.358±0.134
$\Delta t$ 0.01					
VDP [7]	0.559±0.488	0.642±0.577	0.270±0.142	0.209±0.169	0.170±0.152
CVI-DP (Ours)	0.361±0.240	0.154±0.146	0.100±0.131	0.180±0.218	-0.048±0.083
$\Delta t$ 0.005					
VDP [7]	0.385±0.233	0.218±0.184	0.223±0.149	0.162±0.183	0.085±0.141
CVI-DP (Ours)	0.361±0.239	0.154±0.146	0.098±0.134	0.177±0.214	-0.052±0.079
$\Delta t$ 0.001					
VDP [7]	0.374±0.239	0.209±0.191	0.297±0.185	0.165±0.197	0.028±0.133
CVI-DP (Ours)	0.361±0.239	0.154±0.147	0.100±0.135	0.177±0.213	-0.044±0.081

## 4 Experiments

We implement both CVI-DP and VDP within the MarkovFlow [3] framework built on top of TensorFlow [1] and perform a series of experiments to showcase various properties of these methods. For inference and learning, we evaluate the performance of these methods on inference problems covering a set of diffusion process priors, both linear and non-linear, each with its own characteristics (Sec. 4.1). For inference, we show the proposed method CVI-DP performs better than VDP and is at par with the sequential Monte Carlo baseline. For learning, we use the same setup but also learn the model parameters of the DP prior. We show how CVI-DP provides a better learning objective leading to faster learning. Furthermore, to showcase the applicability of CVI-DP in the real world, we demonstrate inference on finance and GPS tracking data sets. (Sec. 4.2).

### 4.1 Evaluation of approximate inference on synthetic problems

We comparatively evaluate our method on synthetic inference problems covering an array of DP priors: the linear DP (Ornstein–Uhlenbeck, OU, Fig. 3),  $dx_t = -\theta x_t dt + d\beta_t$ , as a sanity check for which the posterior process can be written in closed-form; the Beneš DP,  $dx_t = \theta \tanh(x_t) dt + d\beta_t$ , whose marginal state distributions are bimodal and mode-switching in sample state trajectories becomes increasingly unlikely with time (Fig. 7); the double-well (DW) DP,  $dx_t = \theta_0 x_t (\theta_1 - x_t^2) dt + d\beta_t$ , whose marginal state distributions have two modes that sample state trajectories keep visiting through time (Fig. 4); a Sine DP,  $dx_t = \theta_0 \sin(x_t - \theta_1) dt + d\beta_t$ , whose marginal state distributions have many modes (Fig. 8); and a Square-root DP,  $dx_t = \sqrt{\theta} |x_t| dt + d\beta_t$ , that has divergent fat-tailed behaviour (Fig. 9).

**Baselines** As a baseline, we use sequential Monte Carlo (SMC) as particle smoothing through conditional particle filtering with ancestor sampling adopted from [55]. The ‘optimal’ Gaussian baseline is based on a Gaussian fit to the SMC samples. To approximate the log marginal likelihood, we use annealed importance sampling (AIS, [42]) with a similar setup as in [35, 44] (details in App. G).

**Speeding up inference** We compare the performance of approximate inference using VDP and CVI-DP on three aspects: convergence speed, accuracy of the posterior approximation, and robustness to the discretization of the time horizon. As a sanity check, we start with a linear DP prior, where CVI-DP reaches the optimal posterior after a single iteration (Fig. 3). Also, for non-linear DP priors, CVI-DP is faster than VDP (see Fig. 4 for an example with DW prior). Convergence plots for other DPs are available in App. H. To measure the accuracy of the approximate posterior, we use negative log predictive density (NLPD) with 5-fold cross-validation (results in Table 1). The proposed method CVI-DP is robust to the discretization of the time horizon; we report both the methods with different discretization ( $\Delta t = \{0.01, 0.005, 0.001\}$ ). A coarse grid leads to a model with less parameters as the number of variational parameters scales inversely with the discretization step  $\Delta t$ .

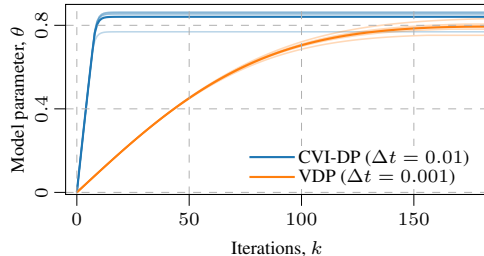


Figure 5: Faster learning of the double-well DP parameter  $\theta$  (M-Step) of the proposed method CVI-DP as compared to VDP.

**Learning of model parameters** To showcase the learning capability of CVI-DP, we experiment with the same setup as in the evaluation of inference but now learn parameters of the prior DP  $\theta$  as well. We compare the two methods on two aspects: speed of learning and posterior predictive accuracy. CVI-DP provides a better objective for learning (Fig. 2) which leads to a faster learning algorithm (Fig. 5). We also report the posterior predictive performance of the methods in Table 2 using NLPD with 5-fold cross-validation as a metric.

**Further comparisons** Finally, we compare against the popular class of NeuralSDEs methods [36, 33]. These methods are variational inference algorithms with a broader scope than CVI-DP: the posterior process  $q$  is not restricted to be a linear DP. However, they rely on sample-based estimation of the ELBO gradient and thus incur a large computational cost and convergence of optimization via stochastic gradient descent is often slow (see App. H.4).

## 4.2 Empirical evaluation on finance and vehicle tracking data

We showcase the learning capability of CVI-DP on real-world data set: finance and vehicle tracking data from [53]. For both data sets, we parameterize the prior DP drift  $f_p$  as an MLP neural network [26], with one hidden layer of 3 nodes and ReLU activation function [24], and learn its parameters.

**Finance data** We model the trend of the share price of Apple Inc. (8537 trading days). We experiment with three models under 5-fold cross-validation: Sparse GP regression model with 500 inducing points [57] and a sum kernel of  $\text{Const.} + \text{Lin.} + \text{Matérn}^{-1/2} + \text{Matérn}^{-3/2}$  as in [53] which gives NLPD  $1.44 \pm 0.70$  / RMSE  $0.91 \pm 0.54$ ; CVI-DP with a linear DP (OU) which gives NLPD  $1.08 \pm 0.45$  / RMSE  $0.77 \pm 0.41$ ; and CVI-DP with a neural network drift DP which gives NLPD  $0.81 \pm 0.08$  / RMSE  $0.51 \pm 0.08$ . The models have different priors incorporated in the form of kernel and prior DP, giving different flexibility to the resulting variational posterior. The aim is to learn the underlying process of the stock price, which we measure in terms of NLPD on the hold-out set. Of all the models, CVI-DP with a NN as drift  $f_p$  results in the best NLPD value as it is the most flexible. Fig. 6 shows simulated predictions from the learnt prior DP (details in App. H.2).

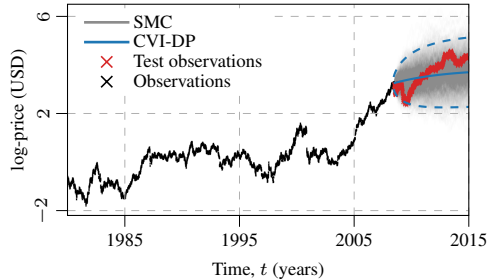


Figure 6: Demonstration on Apple Inc. stock price data set. CVI-DP learns the drift as an MLP neural net and predict into the future.

**Vehicle tracking** We model a 2D trajectory of vehicle movement from GPS coordinates recorded over time. The data set consists of 6373 observation points collected over 106 minutes. Outputs are modelled with two independent DPs learned jointly. Similar to the setup in [53], we split the data in chunks of 30 s and perform 10-fold cross-validation. We experiment with two models: CVI-DP with a NN drift DP which gives NLPD  $-0.82 \pm 0.43$  / RMSE  $0.06 \pm 0.03$ , and CVI-DP with a linear DP (OU), which gives NLPD  $-0.67 \pm 0.19$  / RMSE  $0.13 \pm 0.04$ . CVI-DP with a NN drift gives better NLPD and RMSE value primarily because of the flexibility of the DP to model the trajectory (details in App. H.3).

## 5 Discussion and conclusion

CVI-DP provides a principled and scalable approach for variational inference in models with latent non-linear diffusion processes, parameterized via a time-variant linear Itô SDE. We argue that the Gaussian VI approach commonly used for inference in GP models can readily be extended to the DP prior setting, and propose a unifying approach for both the GP and DP prior settings. Our work fixes practical problems in the seminal work by Archambeau et al. [7] (*cf.* Figs. 2 to 4), and provides an important building block for approximative inference and learning under diffusion processes.

While we tackle the core SDE tooling, diffusion processes have recently gained traction in fields across machine learning such as image generation [28, 54, 16], reinforcement learning [29], and time-series modelling [60, 56, 46]. We see that our work can be an important component in future methods and extended to handle more complex scenarios with additional constraints or priors.

## References

- [1] M. Abadi, A. Agarwal, P. Barham, E. Brevdo, Z. Chen, C. Citro, G. S. Corrado, A. Davis, J. Dean, M. Devin, S. Ghemawat, I. Goodfellow, A. Harp, G. Irving, M. Isard, Y. Jia, R. Jozefowicz, L. Kaiser, M. Kudlur, J. Levenberg, D. Mané, R. Monga, S. Moore, D. Murray, C. Olah, M. Schuster, J. Shlens, B. Steiner, I. Sutskever, K. Talwar, P. Tucker, V. Vanhoucke, V. Vasudevan, F. Viégas, O. Vinyals, P. Warden, M. Wattenberg, M. Wicke, Y. Yu, and X. Zheng. TensorFlow: Large-scale machine learning on heterogeneous systems, 2015. URL <https://www.tensorflow.org/>.
- [2] V. Adam, P. Chang, M. E. E. Khan, and A. Solin. Dual parameterization of sparse variational Gaussian processes. In *Advances in Neural Information Processing Systems 34 (NeurIPS)*, pages 11474–11486. Curran Associates, Inc., 2021.
- [3] V. Adam, A. Artemev, N. Durrande, S. Eleftheriadis, A. Hayes, J. Hensman, J. Jennings, S. John, J. A. Leedham, J. A. McLeod, A. Saul, P. Verma, Y. Wei, and S. Willis. Markovflow, 2022. URL <https://github.com/secondmind-labs/markovflow>.
- [4] S. I. Amari. Natural gradient works efficiently in learning. *Neural Computation*, 10(2):251–276, 1998.
- [5] C. Andrieu, A. Doucet, and R. Holenstein. Particle Markov chain Monte Carlo methods. *Journal of the Royal Statistical Society: Series B (Statistical Methodology)*, 72(3):269–342, 2010.
- [6] C. Archambeau and M. Opper. *Approximate Inference for Continuous-Time Markov Processes*, pages 125–140. Cambridge University Press, 2011.
- [7] C. Archambeau, D. Cornford, M. Opper, and J. Shawe-Taylor. Gaussian process approximations of stochastic differential equations. In *Gaussian Processes in Practice*, volume 1 of *Proceedings of Machine Learning Research*, pages 1–16. PMLR, 2007.
- [8] C. Archambeau, M. Opper, Y. Shen, D. Cornford, and J. Shawe-taylor. Variational inference for diffusion processes. In *Advances in Neural Information Processing Systems (NIPS)*, pages 17–24. Curran Associates, Inc., 2007.
- [9] D. M. Blei, A. Kucukelbir, and J. D. McAuliffe. Variational inference: A review for statisticians. *Journal of the American Statistical Association*, 112(518):859–877, 2017.
- [10] M. Y. Byron, K. V. Shenoy, and M. Sahani. Derivation of Kalman filtering and smoothing equations. Technical report, Stanford University, 2004.
- [11] E. Challis and D. Barber. Gaussian Kullback-Leibler approximate inference. *Journal of Machine Learning Research*, 14:2239–2286, 2013.
- [12] P. E. Chang, W. J. Wilkinson, M. E. Khan, and A. Solin. Fast variational learning in state-space Gaussian process models. In *Proceedings of the 30th International Workshop on Machine Learning for Signal Processing (MLSP)*, pages 1–6. IEEE, 2020.
- [13] R. T. Chen, Y. Rubanova, J. Bettencourt, and D. K. Duvenaud. Neural ordinary differential equations. In *Advances in Neural Information Processing Systems 31 (NeurIPS)*, pages 6571–6583, 2018.
- [14] N. Chopin, O. Papaspiliopoulos, et al. *An Introduction to Sequential Monte Carlo*. Springer, 2020.
- [15] L. Csató and M. Opper. Sparse on-line Gaussian processes. *Neural Computation*, 14(3):641–668, 2002.
- [16] P. Dhariwal and A. Q. Nichol. Diffusion models beat GANs on image synthesis. In *Advances in Neural Information Processing Systems 35 (NeurIPS)*, pages 8780–8794. Curran Associates, Inc., 2021.
- [17] L. Duncker, G. Böhner, J. Boussard, and M. Sahani. Learning interpretable continuous-time models of latent stochastic dynamical systems. In *Proceedings of the 36th International Conference on Machine Learning (ICML)*, volume 97 of *Proceedings of Machine Learning Research*, pages 1726–1734. PMLR, 2019.
- [18] B. Eraker. MCMC analysis of diffusion models with application to finance. *Journal of Business & Economic Statistics*, 19:177–191, 2001.
- [19] C. A. García, A. Otero, P. Félix, J. Presedo, and D. G. Márquez. Nonparametric estimation of stochastic differential equations with sparse Gaussian processes. *Physical Review E*, 96, 2017.
- [20] Á. F. García-Fernández, L. Svensson, M. R. Morelande, and S. Särkkä. Posterior linearization filter: Principles and implementation using sigma points. *IEEE Transactions on Signal Processing*, 63(20): 5561–5573, 2015.

- [21] Á. F. García-Fernández, L. Svensson, and S. Särkkä. Iterated posterior linearization smoother. *IEEE Transactions on Automatic Control*, 62(4):2056–2063, 2016.
- [22] Á. F. García-Fernández, F. Tronarp, and S. Särkkä. Gaussian process classification using posterior linearization. *IEEE Signal Processing Letters*, 26(5):735–739, 2019.
- [23] I. Girsanov. On transforming a certain class of stochastic processes by absolutely continuous substitution of measures. *Theory of Probability and Its Applications*, 5:314–330, 1960.
- [24] X. Glorot, A. Bordes, and Y. Bengio. Deep sparse rectifier neural networks. In *Proceedings of the Fourteenth International Conference on Artificial Intelligence and Statistics (AISTATS)*, volume 15 of *Proceedings of Machine Learning Research*, pages 315–323. PMLR, 2011.
- [25] A. Golightly and D. J. Wilkinson. Bayesian parameter inference for stochastic biochemical network models using particle Markov chain Monte carlo. *Interface Focus*, 1:807–820, 2011.
- [26] I. Goodfellow, Y. Bengio, and A. Courville. *Deep Learning*. MIT Press, 2016.
- [27] M. C. Higgs. *Approximate Inference for State-Space Models*. PhD thesis, University College London, London, UK, 2011.
- [28] J. Ho, A. Jain, and P. Abbeel. Denoising diffusion probabilistic models. In *Advances in Neural Information Processing Systems 33 (NeurIPS)*, pages 6840–6851. Curran Associates, Inc., 2020.
- [29] M. Janner, Y. Du, J. B. Tenenbaum, and S. Levine. Planning with diffusion for flexible behavior synthesis. In K. Chaudhuri, S. Jegelka, L. Song, C. Szepesvári, G. Niu, and S. Sabato, editors, *International Conference on Machine Learning (ICML)*, volume 162, pages 9902–9915. PMLR, 2022.
- [30] I. Karatzas and S. E. Shreve. Brownian motion. In *Brownian Motion and Stochastic Calculus*, pages 47–127. Springer, 1998.
- [31] M. E. Khan and W. Lin. Conjugate-computation variational inference: Converting variational inference in non-conjugate models to inferences in conjugate models. In *Proceedings of the 20th International Conference on Artificial Intelligence and Statistics (AISTATS)*, volume 54 of *Proceedings of Machine Learning Research*, pages 878–887. PMLR, 2017.
- [32] M. E. Khan and D. Nielsen. Fast yet simple natural-gradient descent for variational inference in complex models. In *2018 International Symposium on Information Theory and Its Applications (ISITA)*, pages 31–35. IEEE, 2018.
- [33] P. Kidger, J. Foster, X. C. Li, and T. Lyons. Efficient and accurate gradients for neural SDEs. In *Advances in Neural Information Processing Systems 34 (NeurIPS)*, pages 18747–18761. Curran Associates, Inc., 2021.
- [34] L. Köhs, B. Alt, and H. Koepl. Variational inference for continuous-time switching dynamical systems. In *Advances in Neural Information Processing Systems 34 (NeurIPS)*, volume 34, pages 20545–20557. Curran Associates, Inc., 2021.
- [35] M. Kuss and C. E. Rasmussen. Assessing approximate inference for binary Gaussian process classification. *Journal of Machine Learning Research (JMLR)*, 6:1679–1704, 2005.
- [36] X. Li, T.-K. L. Wong, R. T. Q. Chen, and D. Duvenaud. Scalable gradients for stochastic differential equations. In *Proceedings of the Twenty Third International Conference on Artificial Intelligence and Statistics*, volume 108 of *Proceedings of Machine Learning Research*, pages 3870–3882. PMLR, 2020.
- [37] X. Li, T.-K. L. Wong, R. T. Q. Chen, and D. K. Duvenaud. Scalable gradients and variational inference for stochastic differential equations. In *Proceedings of The 2nd Symposium on Advances in Approximate Bayesian Inference*, volume 118 of *Proceedings of Machine Learning Research*, pages 1–28. PMLR, 2020.
- [38] W. Lin, M. E. Khan, and M. Schmidt. Fast and simple natural-gradient variational inference with mixture of exponential-family approximations. In *Proceedings of the 36th International Conference on Machine Learning (ICML)*, volume 97 of *Proceedings of Machine Learning Research*, pages 3992–4002. PMLR, 2019.
- [39] F. Lindsten, M. I. Jordan, and T. B. Schon. Particle Gibbs with ancestor sampling. *Journal of Machine Learning Research (JMLR)*, 15:2145–2184, 2014.
- [40] T. P. Minka. Expectation propagation for approximate Bayesian inference. In *Proceedings of the 17th Conference in Uncertainty in Artificial Intelligence*, pages 362–369. Morgan Kaufmann, 2001.

- [41] T. P. Minka. *A Family of Algorithms for Approximate Bayesian Inference*. PhD thesis, Massachusetts Institute of Technology, 2001.
- [42] R. M. Neal. Annealed importance sampling. *Statistics and Computing*, 11:125–139, 2001.
- [43] R. M. Neal and G. E. Hinton. A view of the EM algorithm that justifies incremental, sparse, and other variants. In *Learning in Graphical Models*, pages 355–368. Springer, 1998.
- [44] H. Nickisch and C. E. Rasmussen. Approximations for binary Gaussian process classification. *Journal of Machine Learning Research (JMLR)*, 9:2035–2078, 2008.
- [45] B. Øksendal. *Stochastic Differential Equations: An Introduction with Applications*. Springer, New York, NY, sixth edition, 2003.
- [46] S. W. Park, K. Lee, and J. Kwon. Neural Markov controlled SDE: Stochastic optimization for continuous-time data. In *International Conference on Learning Representations (ICLR)*, 2022.
- [47] C. E. Rasmussen and C. K. I. Williams. *Gaussian Processes for Machine Learning*. MIT Press, 2006.
- [48] Y. Rubanova, R. T. Chen, and D. K. Duvenaud. Latent ordinary differential equations for irregularly-sampled time series. In *Advances in Neural Information Processing Systems 32 (NeurIPS)*, pages 5320–5330. Curran Associates, Inc., 2019.
- [49] A. Ruttor, P. Batz, and M. Opper. Approximate Gaussian process inference for the drift function in stochastic differential equations. In *Advances in Neural Information Processing Systems 26 (NIPS)*, pages 2040–2048. Curran Associates, Inc., 2013.
- [50] T. Ryder, A. Golightly, A. S. McGough, and D. Prangle. Black-box variational inference for stochastic differential equations. In *Proceedings of the 35th International Conference on Machine Learning (ICML)*, volume 80 of *Proceedings of Machine Learning Research*, pages 4423–4432. PMLR, 2018.
- [51] S. Särkkä and A. Solin. *Applied Stochastic Differential Equations*. Cambridge University Press, 2019.
- [52] M.-A. Sato. Online model selection based on the variational Bayes. *Neural Computation*, 13(7):1649–1681, 2001.
- [53] A. Solin and S. Särkkä. State space methods for efficient inference in Student-t process regression. In *Proceedings of the Eighteenth International Conference on Artificial Intelligence and Statistics (AISTATS)*, volume 38 of *Proceedings of Machine Learning Research*, pages 885–893. PMLR, 2015.
- [54] Y. Song, C. Durkan, I. Murray, and S. Ermon. Maximum likelihood training of score-based diffusion models. In *Advances in Neural Information Processing Systems 35 (NeurIPS)*, pages 1415–1428. Curran Associates, Inc., 2021.
- [55] A. Svensson, T. B. Schön, and M. Kok. Nonlinear state space smoothing using the conditional particle filter. In *Proceedings of the 17th IFAC Symposium on System Identification (SYSID)*, volume 48, pages 975–980. Elsevier, 2015.
- [56] Y. Tashiro, J. Song, Y. Song, and S. Ermon. CSDI: Conditional score-based diffusion models for probabilistic time series imputation. In *Advances in Neural Information Processing Systems 35 (NeurIPS)*, pages 24804–24816. Curran Associates, Inc., 2021.
- [57] M. Titsias. Variational learning of inducing variables in sparse Gaussian processes. In *Proceedings of the Twelfth International Conference on Artificial Intelligence and Statistics (AISTATS)*, volume 5 of *Proceedings of Machine Learning Research*, pages 567–574. PMLR, 2009.
- [58] F. Tronarp, A. F. Garcia-Fernandez, and S. Särkkä. Iterative filtering and smoothing in nonlinear and non-Gaussian systems using conditional moments. *IEEE Signal Processing Letters*, 25(3):408–412, 2018.
- [59] N. G. Van Kampen. *Stochastic Processes in Physics and Chemistry*, volume 1. Elsevier, 1992.
- [60] F. Vargas, P. Thodoroff, A. Lamacraft, and N. Lawrence. Solving Schrödinger bridges via maximum likelihood. *Entropy*, 23(9):1134, 2021.
- [61] N. Whiteley. Discussion on particle Markov chain Monte Carlo methods. *Journal of the Royal Statistical Society: Series B*, 72(3):306–307, 2010.
- [62] W. J. Wilkinson, S. Särkkä, and A. Solin. Bayes–Newton methods for approximate Bayesian inference with PSD guarantees. *Journal of Machine Learning Research (JMLR)*, 24(83):1–50, 2023.
- [63] C. Yildiz, M. Heinonen, J. Intosalmi, H. Mannerstrom, and H. Lahdesmaki. Learning stochastic differential equations with Gaussian processes without gradient matching. In *2018 IEEE 28th International Workshop on Machine Learning for Signal Processing (MLSP)*, 2018.

---

## Supplementary Material: Variational Gaussian Process Diffusion Processes

---

This supplementary document is organized as follows. App. A describes exact inference for latent diffusion models, and highlights the properties of the posterior drift function. App. B describes an (intractable) variational algorithm to perform exact inference in latent diffusion models, using the method of Lagrangian multipliers to optimize a constrained objective. App. C provides the full derivations for the tractable variational algorithm of Archambeau et al. [7], where the variational distribution is restricted to a set of Markovian Gaussian Process. In App. D, we propose an alternative parameterization for Markovian Gaussian processes by introducing continuous exponential family description. In App. E we derive the Kullback–Leibler divergence between two diffusion processes which is essential for many algorithms including variational inference. App. F provides derivations of the proposed method CVI-DP. App. G gives details about the Monte Carlo baselines and App. H provides details about the experiment setup and insights about various results.

### A Exact inference for latent diffusion process models

In this section, we describe the exact posterior inference in models with diffusion process prior, following the derivations in [27]. Given the Markovian structure of the diffusion, the marginal posterior at time  $t$  factorizes as

$$p(\mathbf{x}_t | \mathcal{D}) = \underbrace{p(\mathbf{x}_t | \mathcal{D}_{<t})}_{p_t^{(F)}(\mathbf{x}_t)} \underbrace{\frac{p(\mathcal{D}_{\geq t} | \mathbf{x}_t)}{p(\mathcal{D}_{\geq t} | \mathcal{D}_{<t})}}_{\psi_t(\mathbf{x}_t)}. \quad (23)$$

This expression splits the contribution of observations before and after time  $t$  into two terms corresponding to continuous time equivalent of the forward and backward (up to a constant) filtering distributions in discrete Markov chains [10].

The forward filtering distribution  $p_t^{(F)}$  satisfies, in between observation times, the Kolmogorov forward equation [30]

$$(\partial_t - \vec{K}_f)p_t^{(F)} = 0, \quad (24)$$

where  $\vec{K}_f$  is the Fokker–Planck operator defined for twice differentiable functions  $\phi$  as

$$\vec{K}_f[\phi(\mathbf{x})] := -\nabla^\top [f(\mathbf{x}, t)\phi(\mathbf{x})] + \frac{1}{2}\text{tr}(\mathbf{Q}_c(\nabla\nabla^\top)[\phi(\mathbf{x})]). \quad (25)$$

Similarly, the second term  $\psi_t(\mathbf{x}_t)$ —also known as the information filter—satisfies, in between observation times, the Kolmogorov backward equation

$$(\partial_t + \overleftarrow{K}_f)\psi_t = 0, \quad (26)$$

where  $\overleftarrow{K}_f$  is the adjoint of the Fokker–Planck operator defined for twice differentiable functions  $\phi$  as

$$\overleftarrow{K}_f[\phi(\mathbf{x})] := f(\mathbf{x}, t)^\top \nabla[\phi(\mathbf{x})] + \frac{1}{2}\text{tr}(\mathbf{Q}_c(\nabla\nabla^\top)[\phi(\mathbf{x})]). \quad (27)$$

If solving for  $p_t^{(F)}$  forward in time, at the discrete observation times  $t$ , observations are added from the conditioning sets of  $p_t^{(F)}$ , leading to the instantaneous updates

$$p_{t^+}^{(F)}(\mathbf{x}_{t^+}) \propto p_{t^-}^{(F)}(\mathbf{x}_{t^-})p(\mathcal{D}_t | \mathbf{x}_{t^-}). \quad (28)$$

The information filter  $\psi_t$  can be solved backwards with the initial condition  $\psi_T = 1$  and discrete updates

$$\psi_{t^-}(\mathbf{x}_{t^-}) = \frac{p(\mathcal{D}_t | \mathbf{x}_t)\psi_{t^+}(\mathbf{x}_{t^+})}{p(\mathcal{D}_t | \mathcal{D}_{<t})}. \quad (29)$$

Differentiating the marginal posterior distribution  $p_{\mathbf{x}_t | \mathcal{D}}$  through time [27, Theorem 2.8], it can be shown that the posterior process  $p_{\mathbf{x} | \mathbf{y}}$  shares the same diffusion as the prior process and its drift  $h$  is given by:

$$h(\mathbf{x}_t, t) = f_p(\mathbf{x}_t, t) + \mathbf{Q}_c \nabla \log \psi_t(\mathbf{x}_t). \quad (30)$$

This result reveals that the posterior process shares the same Markovian structure as the prior process. It also provides a recipe to compute the posterior marginals: (1) compute  $\psi_t$  backward in time via Eq. (26) and the jump conditions Eq. (29), and (2) compute the posterior drift via Eq. (30) and compute the marginals of the posterior process via Eq. (24). These steps are however intractable for most settings of non-linear drift and observation models.

## B Variational inference for latent diffusion process models (General case)

In this section, we derive the posterior process for latent diffusion models starting from the variational formulation of the problem. We introduce the variational objective, describe an optimization procedure and discuss some properties of the solution.

We start from the variational objective for inference in latent diffusion models given in Eq. (5), which we rewrite here for completeness

$$\mathcal{L}(q) = \mathbb{E}_{q(\mathbf{x})}[\log p(\mathbf{y} | \mathbf{x})] - \frac{1}{2} \int_0^\tau \mathbb{E}_{q(\mathbf{x}_t)} \|f_q(\mathbf{x}_t, t) - f_p(\mathbf{x}_t, t)\|_{\mathbf{Q}_c^{-1}}^2 dt - \text{D}_{\text{KL}}[q(\mathbf{x}_0) \| p(\mathbf{x}_0)]. \quad (31)$$

The drift  $f_{q^*}$  of the optimal variational process  $q^*$  maximizing  $\mathcal{L}(q)$  can be derived from this variational objective using the tools of Lagrangian duality. Let  $\tilde{\mathcal{L}}(q, f_q)$  be the ELBO defined in Eq. (31) where we have severed the dependency between  $q$  and  $f_q$ . The optimization of the ELBO can be cast as the optimization problem

$$\max_q \tilde{\mathcal{L}}(q, f_q) \quad \text{subject to} \quad [(\partial_t - \vec{K}_{f_q})q](\mathbf{x}, t) = 0, \quad \forall \mathbf{x}, t, \quad (32)$$

where  $\vec{K}_f$  is the Fokker–Planck operator defined in Eq. (25). We introduce the Lagrangian  $\lambda$  associated to this constrained optimization problem

$$\mathfrak{L}(q, f_q, \lambda) = \tilde{\mathcal{L}}(q, f_q) + \int \int \lambda(\mathbf{x}_t, t) [(\partial_t - \vec{K}_{f_q})q](\mathbf{x}_t, t) d\mathbf{x}_t dt. \quad (33)$$

A local optimum  $(q^*, f_q^*)$  of the original constrained optimization problem is associated to a unique pair of Lagrangian multipliers  $\lambda^*$  satisfying  $\nabla_{q, f_q, \lambda} \mathfrak{L}|_{q^*, f_q^*, \lambda^*} = 0$ . Introducing the change of variable  $\lambda(\mathbf{x}, t) = -\log \psi(\mathbf{x}, t)$ , the system of equations can be written as

$$0 = \frac{\partial \psi(\mathbf{x}, t)}{\partial t} + \overleftarrow{K}_f[\psi(\mathbf{x}, t)] + \psi(\mathbf{x}, t) \sum_{i=1}^N [\log p(\mathbf{y}_i | \mathbf{x}_i)] \delta(t - t_i). \quad (34)$$

We recover the posterior drift as in Eq. (30),

$$f_q(\mathbf{x}_t, t) = f_p(\mathbf{x}_t, t) + \mathbf{Q}_c \nabla \log \psi(\mathbf{x}_t, t). \quad (35)$$

## C Gaussian variational inference for diffusion processes (VDP)

In this section, we focus on the case where the set of variational processes is restricted to that of Markovian Gaussian processes, as described in Sec. 2.1. More formally, the variational process  $q$  is restricted to be a diffusion with an affine drift

$$\mathcal{Q} = \{q : d\mathbf{x}_t = (\mathbf{A}_t \mathbf{x}_t + \mathbf{b}_t) dt + \mathbf{L} d\beta_t, \quad \mathbf{x}_0 \sim q(\mathbf{x}_0)\}. \quad (36)$$

The drift parameters  $\mathbf{A}_t \in \mathbb{R}^{d \times d}$  and  $\mathbf{b}_t \in \mathbb{R}^d$  are associated to a unique set of marginal distributions  $q(\mathbf{x}_t)$ , which are fully characterised by the mean and covariance  $\mathbf{M} = (\mathbf{m}_t, \mathbf{S}_t)$ . We denote by  $\mathbf{V} = (\mathbf{A}_t, \mathbf{b}_t)$  the *variational* parameters of  $q$ . The ELBO is given by

$$\mathcal{L}(\mathbf{M}, \mathbf{V}) = \mathbb{E}_{q(\mathbf{x})} \log p(\mathbf{y} | \mathbf{x}) + \frac{1}{2} \int_0^T \mathbb{E}_{q(\mathbf{x}_t)} \|(\mathbf{A}_t \mathbf{x}_t + \mathbf{b}_t) - f_p(\mathbf{x}_t, t)\|_{\mathbf{Q}_c^{-1}}^2 dt - \text{D}_{\text{KL}}[q(\mathbf{x}_0) \| p(\mathbf{x}_0)]. \quad (37)$$

The constraints connecting the drift parameters to the marginal statistics  $(\mathbf{m}, \mathbf{S})$  are

$$C[\mathbf{M}, \mathbf{V}](t) = \begin{bmatrix} \dot{\mathbf{m}}_t - \mathbf{A}_t \mathbf{m}_t - \mathbf{b}_t \\ \dot{\mathbf{S}}_t - \mathbf{A}_t \mathbf{S}_t - \mathbf{S}_t \mathbf{A}_t^\top - \mathbf{Q}_c \end{bmatrix} = \mathbf{0} \quad \forall t. \quad (38)$$

The constrained optimization problem is thus

$$\max_{\mathbf{M}, \mathbf{V}} \mathcal{L}(\mathbf{M}, \mathbf{V}) \quad (39)$$

$$\text{subject to } C[\mathbf{M}, \mathbf{V}](t) = \mathbf{0} \quad \forall t. \quad (40)$$

A Lagrangian is constructed, with Lagrangian multipliers  $\Theta = (\boldsymbol{\lambda}_t, \boldsymbol{\Psi}_t)$  associated to each of the two constraints as

$$\mathfrak{L}(\mathbf{M}, \mathbf{V}, \Theta) = \mathcal{L}(\mathbf{M}, \mathbf{V}) - \int_0^T \langle \Theta, C[\mathbf{M}, \mathbf{V}](t) \rangle dt. \quad (41)$$

A local optimum  $(\mathbf{M}^*, \mathbf{V}^*)$  of the original constrained optimization problem is associated to a unique pair of Lagrangian multipliers  $\Theta^*$  satisfying  $\nabla_{\mathbf{M}_t, \mathbf{V}_t, \Theta_t} \mathfrak{L}|_{\mathbf{M}_t^*, \mathbf{V}_t^*, \Theta_t^*} = 0, \forall t$ . The system of equations can be re-expressed as:

$$\dot{\boldsymbol{\Psi}}_t^* = -\mathbf{A}_t^{*\top} \boldsymbol{\Psi}_t^* - \boldsymbol{\Psi}_t^* \mathbf{A}_t^* - \nabla_{\mathbf{S}} \mathcal{L}|_{\mathbf{S}^*}, \quad (42)$$

$$\dot{\boldsymbol{\lambda}}_t^* = -\mathbf{A}_t^{*\top} \boldsymbol{\lambda}_t^* - \nabla_{\mathbf{m}} \mathcal{L}|_{\mathbf{m}^*}, \quad (43)$$

$$\mathbf{A}_t^* = \mathbb{E}_{q^*}[\nabla_{\mathbf{x}} f] - 2\mathbf{Q}_c \boldsymbol{\Psi}_t^*, \quad (44)$$

$$\mathbf{b}_t^* = \mathbb{E}_{q^*}[f] - \mathbf{A}_t^* \mathbf{m}_t^* - \boldsymbol{\lambda}_t^*, \quad (45)$$

$$0 = C[\mathbf{m}^*, \mathbf{S}^*, \mathbf{A}^*, \mathbf{b}^*]. \quad (46)$$

### C.1 Fixed point iterations

The system of equations derived earlier are not analytically solvable. They consist of self consistency equations among the optimal variables  $\mathbf{x}_t^*, \Theta_t^*$ . To find optimal solutions to this problem, a fixed point algorithm, whereby a sequence of variables  $(\mathbf{x}_t^{(k)}, \Theta_t^{(k)})$  is constructed in [7] using the self consistency equations as follows:

$$\text{From Eq. (42): } \boldsymbol{\Psi}^{(k+1)} \leftarrow \dot{\boldsymbol{\Psi}}_t = -\mathbf{A}_t^{(k)\top} \boldsymbol{\Psi}_t - \boldsymbol{\Psi}_t \mathbf{A}_t^{(k)} - \nabla_{\mathbf{S}} \mathcal{L}|_{\mathbf{S}^{(k)}}, \text{ with } \boldsymbol{\Psi}(T) = 0, \quad (47)$$

$$\text{From Eq. (43): } \boldsymbol{\lambda}^{(k+1)} \leftarrow \dot{\boldsymbol{\lambda}}_t = -\mathbf{A}_t^{(k)\top} \boldsymbol{\lambda}_t - \nabla_{\mathbf{m}} \mathcal{L}|_{\mathbf{m}^{(k)}}, \text{ with } \boldsymbol{\lambda}(T) = 0, \quad (48)$$

$$\text{From Eq. (44): } \mathbf{A}^{(k+1)} \leftarrow (1 - \omega)\mathbf{A}^{(k)} + \omega(\mathbb{E}_{q^{(k)}}[\nabla_{\mathbf{x}} f] - 2\mathbf{Q}_c \boldsymbol{\Psi}^{(k+1)}), \quad (49)$$

$$\text{From Eq. (45): } \mathbf{b}^{(k+1)} \leftarrow (1 - \omega)\mathbf{b}^{(k)} + \omega(\mathbb{E}_{q^{(k)}}[f] - \mathbf{A}_t^{(k+1)} \mathbf{m}_t^{(k)} - \boldsymbol{\lambda}_t^{(k+1)}), \quad (50)$$

$$\text{From Eq. (46): } \mathbf{m}^{(k+1)} \leftarrow \dot{\mathbf{m}}_t - \mathbf{A}_t^{(k+1)} \mathbf{m}_t - \mathbf{b}_t^{(k+1)}, \quad (51)$$

$$\text{From Eq. (46): } \mathbf{S}^{(k+1)} \leftarrow \dot{\mathbf{S}}_t - \mathbf{A}_t^{(k+1)} \mathbf{S}_t - \mathbf{S}_t \mathbf{A}_t^{(k+1)\top} - \mathbf{Q}_c. \quad (52)$$

The iterations are run until convergence. In Eqs. (49) and (50), the learning-rate  $\omega$  is introduced for stability reason. It enforces a degree of stickiness to the previous values for  $\mathbf{A}$  and  $\mathbf{b}$  in the sequence defined by the updates.

## D Exponential family for Markovian Gaussian processes

We propose an alternative parameterization for Markovian Gaussian processes by introducing a continuous exponential family description of such processes. This description corresponds to the continuous time limit of the exponential family characterization of discrete Gaussian Markov chains.

### D.1 Linear Gaussian discrete Markov chains

We first consider a Linear Gaussian discrete Markov chain, also known as linear Gaussian state space model (LGSSM), which specifies the distribution of a finite collection of random variables  $\mathbf{x} = [\mathbf{x}_0, \dots, \mathbf{x}_N]$  as follows:

$$\mathbf{x}_0 \sim \mathcal{N}(\mathbf{m}_0, \mathbf{S}_0), \quad (53)$$

$$\mathbf{x}_{i+1} = \hat{\mathbf{A}}_i \mathbf{x}_i + \hat{\mathbf{b}}_i + \hat{\varepsilon}_i, \quad \hat{\varepsilon}_i \sim \mathcal{N}(\mathbf{0}, \hat{\mathbf{Q}}_i). \quad (54)$$

The joint density over  $\mathbf{x}$  factorises as a chain  $p(\mathbf{x}_0, \dots, \mathbf{x}_N) = p(\mathbf{x}_0) \prod_{i=1}^N p(\mathbf{x}_i | \mathbf{x}_{i-1})$ . It is common in the literature to parametrize the ‘drift’ via statistics  $\boldsymbol{\varphi} = \{\hat{\mathbf{A}}_i, \hat{\mathbf{b}}_i, \hat{\mathbf{Q}}_i\}_{i=1}^N$ . It provides an intuitive description of the collection as a temporal process and also an effective way to compute the marginal means  $\mathbf{m}_i$ , covariances  $\mathbf{S}_i$  and cross covariances  $\mathbf{C}_i$ , defined as

$$\mathbf{m}_{i+1} = \mathbb{E}[\mathbf{x}_{i+1}] = \hat{\mathbf{A}}_i \mathbf{m}_i + \hat{\mathbf{b}}_i, \quad (55)$$

$$\mathbf{S}_{i+1} = \mathbb{E}[(\mathbf{x}_{i+1} - \mathbf{m}_{i+1})(\mathbf{x}_{i+1} - \mathbf{m}_{i+1})^\top] = \hat{\mathbf{A}}_i \mathbf{S}_i \hat{\mathbf{A}}_i^\top + \hat{\mathbf{Q}}_i, \quad (56)$$

$$\mathbf{C}_i = \mathbb{E}[(\mathbf{x}_{i+1} - \mathbf{m}_{i+1})(\mathbf{x}_i - \mathbf{m}_i)^\top] = \hat{\mathbf{A}}_i \mathbf{S}_i. \quad (57)$$

The stacked parameters  $\mathbf{M} = \{\mathbf{m}_i, \mathbf{S}_{i+1}, \mathbf{C}_{i+1}\}_{i=1}^N$  constitute a parameterization of the LGSSM. A convenient alternative parameterization of LGSSMs is as a special case of conditional exponential family distributions [38]

$$p(\mathbf{x}_{i+1} | \mathbf{x}_i) = \exp[\langle \mathbb{T}_c(\mathbf{x}_{i+1}, \mathbf{x}_i), \boldsymbol{\lambda}_i \rangle - A_c(\boldsymbol{\lambda}_i)], \quad (58)$$

$$p(\mathbf{x}_0) = \exp[\langle \mathbb{T}(\mathbf{x}_0), \boldsymbol{\lambda}_0 \rangle - A(\boldsymbol{\lambda}_0)], \quad (59)$$

where for each conditional distribution,  $\mathbb{T}_c(\mathbf{x}_{i+1}, \mathbf{x}_i)$  are the sufficient statistics,  $\boldsymbol{\lambda}_i$  the natural parameters, and  $A_c(\boldsymbol{\lambda}_i)$  the associated log partition function.

The initial state is distributed as a multivariate Gaussian with sufficient statistics and natural parameters

$$\mathbb{T}(\mathbf{x}_0) = [\mathbf{x}_0, \mathbf{x}_0 \mathbf{x}_0^\top]; \quad \boldsymbol{\lambda}_0 = [\mathbf{S}_0^{-1} \mathbf{m}_0, -\frac{1}{2} \mathbf{S}_0^{-1}]. \quad (60)$$

By expanding the log conditional density as

$$\log p(\mathbf{x}_{i+1} | \mathbf{x}_i) = -\frac{1}{2} (\mathbf{x}_{i+1} - \hat{\mathbf{A}}_i \mathbf{x}_i - \hat{\mathbf{b}}_i)^\top \hat{\mathbf{Q}}_i^{-1} (\mathbf{x}_{i+1} - \hat{\mathbf{A}}_i \mathbf{x}_i - \hat{\mathbf{b}}_i) + c \quad (61)$$

$$= \mathbf{x}_{i+1}^\top \hat{\mathbf{Q}}_i^{-1} \hat{\mathbf{b}}_i - \frac{1}{2} \mathbf{x}_{i+1}^\top \hat{\mathbf{Q}}_i^{-1} \mathbf{x}_{i+1} + \mathbf{x}_{i+1}^\top \hat{\mathbf{Q}}_i^{-1} \hat{\mathbf{A}}_i \mathbf{x}_i + \tilde{c}, \quad (62)$$

we can identify

$$\mathbb{T}(\mathbf{x}_{i+1}, \mathbf{x}_i) = [\mathbf{x}_{i+1}, \mathbf{x}_{i+1} \mathbf{x}_{i+1}^\top, \mathbf{x}_{i+1} \mathbf{x}_i^\top]; \quad \boldsymbol{\lambda}_i = [\hat{\mathbf{Q}}_i^{-1} \hat{\mathbf{b}}_i, -\frac{1}{2} \hat{\mathbf{Q}}_i^{-1}, \hat{\mathbf{Q}}_i^{-1} \hat{\mathbf{A}}_i], \quad (63)$$

where the inner product in Eq. (59) (resp. Eq. (58)) distributes over the sufficient statistics in Eq. (60) (resp. Eq. (63)) and is the standard inner product  $\mathbf{a}, \mathbf{b} \rightarrow \mathbf{a}^\top \mathbf{b}$  for vectors and  $\mathbf{A}, \mathbf{B} \rightarrow \text{Trace}(\mathbf{A}^\top \mathbf{B})$  for matrices.

Finally, the expectation parameters  $\boldsymbol{\mu}$  for the conditional exponential family distribution are defined as

$$\boldsymbol{\mu}_i = \mathbb{E}_{p(\mathbf{x}_{i+1}, \mathbf{x}_i)}[\mathbb{T}(\mathbf{x}_{i+1}, \mathbf{x}_i)] = [\mathbf{m}_{i+1}, \mathbf{S}_{i+1} + \mathbf{m}_{i+1} \mathbf{m}_{i+1}^\top, \mathbf{C}_i + \mathbf{m}_{i+1}], \quad (64)$$

$$\boldsymbol{\mu}_0 = \mathbb{E}_{p(\mathbf{x}_0)}[\mathbb{T}_0(\mathbf{x}_0)] = [\mathbf{m}_0, \mathbf{S}_0 + \mathbf{m}_0 \mathbf{m}_0^\top]. \quad (65)$$

The joint distribution over states  $\mathbf{x}$  is a  $(\mathbb{T} + 1)d$ -dimensional multivariate normal distribution in the exponential family

$$p(\mathbf{x}_0, \dots, \mathbf{x}_N) = \exp[\langle \mathbb{T}(\mathbf{x}), \boldsymbol{\eta}_p \rangle - A(\boldsymbol{\eta}_p)]. \quad (66)$$

Building the joint density by multiplying the terms from the conditional exponential family description (Eq. (59) and Eq. (58)) reveals the sparse structure of the sufficient statistics. Indeed these are the union of the initial and conditional sufficient statistics in Eq. (60) and Eq. (63). Importantly, they only include the outer product of identical states  $\mathbf{x}_i \mathbf{x}_i^\top$  or consecutive states  $\mathbf{x}_i \mathbf{x}_{i+1}^\top$ . These sufficient statistics can be conveniently written as  $\mathbb{T}(\mathbf{x}) = [\mathbf{x}, \text{btd}(\mathbf{x} \mathbf{x}^\top)]$  where  $\text{btd}(\mathbf{M})$  sets entries of  $\mathbf{M}$  outside of the  $d$ -block tri-diagonals to zero.

An important property we use in the paper is that given two such LGSSMs indexed  $p_1, p_2$  with natural parameters  $\boldsymbol{\eta}^{(1)}, \boldsymbol{\eta}^{(2)}$ , the Kullback Leibler divergence is

$$\nabla_{\boldsymbol{\mu}^{(1)}} \text{D}_{\text{KL}} [p_1(\mathbf{x}; \boldsymbol{\eta}^{(1)}) \| p_1(\mathbf{x}; \boldsymbol{\eta}^{(2)})] = \boldsymbol{\eta}^{(1)} - \boldsymbol{\eta}^{(2)}. \quad (67)$$

A LGSSM is fully characterized by either of the parameterizations  $\boldsymbol{\eta}, \boldsymbol{\mu}, \boldsymbol{\varphi}$  and  $\mathbf{M}$ . There is a bijective mapping between each of these parameterizations and CVI-DP requires to compute some of

these transformations, which we derive here for completeness.  
 $\varphi$  to  $\mathbf{M}$

$$\mathbf{A}_i = \mathbf{C}_i \mathbf{S}_i^{-1} \quad (68)$$

$$\mathbf{Q}_i = \mathbf{S}_{i+1} - \mathbf{A}_i \mathbf{S}_i \mathbf{A}_i^\top \quad (69)$$

$$\mathbf{b}_i = \mathbf{m}_{i+1} - \mathbf{A}_i \mathbf{m}_i \quad (70)$$

$\mathbf{M}$  to  $\boldsymbol{\mu}$

$$\boldsymbol{\mu}_i = [\mathbf{m}_{i+1}, \mathbf{S}_{i+1} + \mathbf{m}_{i+1} \mathbf{m}_{i+1}^\top, \mathbf{C}_i + \mathbf{m}_{i+1} \mathbf{m}_i^\top] \quad (71)$$

$$\boldsymbol{\mu}_0 = [\mathbf{m}_0, \mathbf{S}_0 + \mathbf{m}_0 \mathbf{m}_0^\top] \quad (72)$$

$\boldsymbol{\mu}$  to  $\mathbf{M}$

$$[\mathbf{m}_{i+1}, \mathbf{S}_{i+1}, \mathbf{C}_i] = [\boldsymbol{\mu}_i^{(1)}, \boldsymbol{\mu}_i^{(2)} - \boldsymbol{\mu}_i^{(1)} \boldsymbol{\mu}_i^{(1)\top}, \boldsymbol{\mu}_i^{(3)} - \boldsymbol{\mu}_i^{(1)} \boldsymbol{\mu}_{i-1}^{(1)\top}] \quad (73)$$

$$[\mathbf{m}_0, \mathbf{S}_0] = [\boldsymbol{\mu}_0^{(1)}, \boldsymbol{\mu}_0^{(2)} - \mathbf{m}_0 \mathbf{m}_0^\top] \quad (74)$$

$\boldsymbol{\mu}$  to  $\varphi$

$$\mathbf{A}_i = \mathbf{C}_i \mathbf{S}_i^{-1} = (\boldsymbol{\mu}_i^{(3)} - \boldsymbol{\mu}_i^{(1)} \boldsymbol{\mu}_{i-1}^{(1)\top}) (\boldsymbol{\mu}_{i-1}^{(2)} - \boldsymbol{\mu}_{i-1}^{(1)} \boldsymbol{\mu}_{i-1}^{(1)\top})^{-1} \quad (75)$$

$$\mathbf{b}_i = \mathbf{m}_{i+1} - \mathbf{A}_i \mathbf{m}_i = \boldsymbol{\mu}_i^{(1)} - (\boldsymbol{\mu}_i^{(3)} - \boldsymbol{\mu}_i^{(1)} \boldsymbol{\mu}_{i-1}^{(1)\top}) (\boldsymbol{\mu}_{i-1}^{(2)} - \boldsymbol{\mu}_{i-1}^{(1)} \boldsymbol{\mu}_{i-1}^{(1)\top})^{-1} \boldsymbol{\mu}_{i-1}^{(1)} \quad (76)$$

## D.2 Continuous case

In this section, we are interested in the limit case of a diffusion process with linear drift

$$\mathbf{x}_0 \sim \mathcal{N}(\mathbf{m}_0, \mathbf{S}_0), \quad (77)$$

$$d\mathbf{x}_t = (\mathbf{A}_t \mathbf{x}_t + \mathbf{b}_t) dt + d\boldsymbol{\beta}_t, \quad (78)$$

where  $\boldsymbol{\beta}_t$  denotes the Brownian motion with  $\mathbf{Q}_c$  spectral density. In a diffusion process,  $d\mathbf{x}$  represents an infinitesimal state difference  $\mathbf{x}_{t+dt} - \mathbf{x}_t$ .

For such linear diffusions, the marginal mean and covariances can be shown to follow the following ordinary differential equations [51]:

$$\mathbf{x}_t \xrightarrow{\mathbb{E}} \mathbf{m}_t \quad \rightarrow \quad \dot{\mathbf{m}}_t = \mathbf{A}_t \mathbf{m}_t + \mathbf{b}_t, \quad (79)$$

$$(\mathbf{x}_t - \mathbf{m}_t)(\mathbf{x}_t - \mathbf{m}_t)^\top \xrightarrow{\mathbb{E}} \mathbf{P}_t \quad \rightarrow \quad \dot{\mathbf{P}}_t = \mathbf{A}_t \mathbf{P}_t + \mathbf{P}_t \mathbf{A}_t^\top + \mathbf{Q}_c. \quad (80)$$

To match the discrete description, we need the third statistic  $\mathbf{C}_t = \mathbf{P}_t \mathbf{A}_t^\top$ . In a similar vein as in the discrete case, we can view the diffusion process as a conditional exponential family model

$$p(d\mathbf{x}_t | \mathbf{x}_t) = \exp[\langle \mathbf{T}(\mathbf{x}_t, d\mathbf{x}_t), \boldsymbol{\lambda}_t \rangle - A(\boldsymbol{\lambda}_t, \mathbf{x}_t)], \quad (81)$$

with sufficient statistics as

$$\mathbf{T}(\mathbf{x}, d\mathbf{x}) = [\mathbf{x} + d\mathbf{x}, (\mathbf{x} + d\mathbf{x})(\mathbf{x} + d\mathbf{x})^\top, (\mathbf{x} + d\mathbf{x})\mathbf{x}^\top] \quad (82)$$

and natural parameters as

$$\boldsymbol{\lambda}_t = [\mathbf{Q}_c^{-1} \mathbf{b}_t, -\frac{1}{2} (dt \mathbf{Q}_c)^{-1}, (dt \mathbf{Q}_c)^{-1} (\mathbf{I} + \mathbf{A}_t dt)]. \quad (83)$$

Equivalently, we can define the associated expectation parameters as  $\boldsymbol{\mu}_t = \mathbb{E}[\mathbf{T}(\mathbf{x}_t, d\mathbf{x}_t)]$ . Importantly, the property still holds that for two diffusions  $p_1, p_2$  with natural parameters  $\boldsymbol{\eta}^{(1)}, \boldsymbol{\eta}^{(2)}$ , the Kullback–Leibler divergence verifies as

$$\nabla_{\boldsymbol{\mu}^{(1)}} \text{D}_{\text{KL}} [p_1(\mathbf{x}; \boldsymbol{\eta}^{(1)}) \| p_1(\mathbf{x}; \boldsymbol{\eta}^{(2)})] = \boldsymbol{\eta}^{(1)} - \boldsymbol{\eta}^{(2)}. \quad (84)$$

## E Kullback–Leibler divergence between diffusion processes

The Kullback–Leibler (KL) divergence is a commonly used divergence to measure the difference between two distributions. In case of diffusion processes, if both the DPs are linear, they can be described in an equivalent Gaussian process whose KL can be calculated conveniently. In case both DPs have the same diffusion, Girsanov theorem [23] can be used to calculate the KL between them. Formally,

$$p : d\mathbf{x}_t = f_p(\mathbf{x}_t, t) dt + d\beta_t, \quad \mathbf{x}_0 \sim p(\mathbf{x}_0), \quad (85)$$

$$q : d\mathbf{x}_t = f_q(\mathbf{x}_t, t) dt + d\beta_t, \quad \mathbf{x}_0 \sim q(\mathbf{x}_0), \quad (86)$$

and both the processes  $p$  and  $q$  have the Brownian motion  $\beta_t$  with  $\mathbf{Q}_c$  spectral density. Then, the KL between  $q$  and  $p$  can be evaluated as

$$D_{\text{KL}} [q \parallel p] = \frac{1}{2} \int_0^T \mathbb{E}_{q(\mathbf{x}_t)} \|f_q(\mathbf{x}_t, t) - f_p(\mathbf{x}_t, t)\|_{\mathbf{Q}_c^{-1}}^2 dt + D_{\text{KL}} [q(\mathbf{x}_0) \parallel p(\mathbf{x}_0)]. \quad (87)$$

For implementation purposes, we approximate the integral in the KL expression by the Riemann sum

$$D_{\text{KL}} [q \parallel p] \approx \frac{1}{2} \sum_{i=0}^{\lfloor T/\Delta t \rfloor} \mathbb{E}_{q(\mathbf{x}_{i\Delta t})} \|f_q(\mathbf{x}_{i\Delta t}, i\Delta t) - f_p(\mathbf{x}_{i\Delta t}, i\Delta t)\|_{\mathbf{Q}_c^{-1}}^2 \Delta t + D_{\text{KL}} [q(\mathbf{x}_0) \parallel p(\mathbf{x}_0)]. \quad (88)$$

This corresponds to the KL between two finite state space models (SSMs) with adequately chosen transition and noise function. Here, we derive the KL between two finite non-linear SSMs. We consider a single transition for simplicity. Consider the two SSMs:

$$p : \begin{cases} \mathbf{x}_0 \sim N(\mathbf{m}_0^{(p)}, \mathbf{S}_0^{(p)}) \\ \mathbf{x}_1 = f_p(\mathbf{x}_0) + \varepsilon_p \sim N(0, \mathbf{Q}_c^{(p)}), \end{cases} \quad (89)$$

$$q : \begin{cases} \mathbf{x}_0 \sim N(\mathbf{m}_0^{(q)}, \mathbf{S}_0^{(q)}) \\ \mathbf{x}_1 = f_q(\mathbf{x}_0) + \varepsilon_q \sim N(0, \mathbf{Q}_c^{(q)}), \end{cases} \quad (90)$$

Then, the KL between the two SSMs can be written as

$$D_{\text{KL}} [q \parallel p] = \mathbb{E}_q \log \frac{q(\mathbf{x}_0, \mathbf{x}_1)}{p(\mathbf{x}_0, \mathbf{x}_1)}, \quad (91)$$

$$= \mathbb{E}_{q(\mathbf{x}_0)} \log \frac{q(\mathbf{x}_0)}{p(\mathbf{x}_0)} + \mathbb{E}_{q(\mathbf{x}_0, \mathbf{x}_1)} \log \frac{q(\mathbf{x}_1 | \mathbf{x}_0)}{p(\mathbf{x}_1 | \mathbf{x}_0)} \quad (92)$$

$$= D_{\text{KL}} [q(\mathbf{x}_0) \parallel p(\mathbf{x}_0)] + \mathbb{E}_{q(\mathbf{x}_0)} D_{\text{KL}} [q(\mathbf{x}_1 | \mathbf{x}_0) \parallel p(\mathbf{x}_1 | \mathbf{x}_0)]. \quad (93)$$

The second term in Eq. (93) can be splitted as

$$D_{\text{KL}} [q(\mathbf{x}_1 | \mathbf{x}_0) \parallel p(\mathbf{x}_1 | \mathbf{x}_0)] = \mathbb{E}_{q(\mathbf{x}_1 | \mathbf{x}_0)} \log q(\mathbf{x}_1 | \mathbf{x}_0) - \mathbb{E}_{q(\mathbf{x}_1 | \mathbf{x}_0)} \log p(\mathbf{x}_1 | \mathbf{x}_0) \quad (94)$$

$$= -H[q(\mathbf{x}_1 | \mathbf{x}_0)] - \mathbb{E}_{q(\mathbf{x}_1 | \mathbf{x}_0)} \log p(\mathbf{x}_1 | \mathbf{x}_0). \quad (95)$$

We have a closed form formula for the entropy, which is independent of  $\mathbf{x}_0$ :

$$H[q(\mathbf{x}_1 | \mathbf{x}_0)] = \frac{1}{2} \log |2\pi \mathbf{Q}_c^{(q)}| + \frac{d}{2}. \quad (96)$$

For the cross entropy term in Eq. (95), we have

$$\begin{aligned} -2 \mathbb{E}_{q(\mathbf{x}_1 | \mathbf{x}_0)} \log p(\mathbf{x}_1 | \mathbf{x}_0) &= \log |2\pi \mathbf{Q}_c^{(p)}| + \mathbb{E}_{q(\mathbf{x}_1 | \mathbf{x}_0)} \|\mathbf{x}_1 - f_p(\mathbf{x}_0)\|_{\mathbf{Q}_c^{(p)-1}}^2 \\ &= \log |2\pi \mathbf{Q}_c^{(p)}| + \mathbb{E}_{q(\mathbf{x}_1 | \mathbf{x}_0)} \|(\mathbf{x}_1 - f_q(\mathbf{x}_0)) - (f_p(\mathbf{x}_0) - f_q(\mathbf{x}_0))\|_{\mathbf{Q}_c^{(p)-1}}^2 \\ &= \log |2\pi \mathbf{Q}_c^{(p)}| + \mathbb{E}_{q(\mathbf{x}_1 | \mathbf{x}_0)} \left[ \|\mathbf{x}_1 - f_q(\mathbf{x}_0)\|_{\mathbf{Q}_c^{(p)-1}}^2 \right. \\ &\quad \left. + \|f_p(\mathbf{x}_0) - f_q(\mathbf{x}_0)\|_{\mathbf{Q}_c^{(p)-1}}^2 - 2\langle \mathbf{x}_1 - f_q(\mathbf{x}_0), f_p(\mathbf{x}_0) - f_q(\mathbf{x}_0) \rangle_{\mathbf{Q}_c^{(p)-1}} \right] \\ &= \log |2\pi \mathbf{Q}_c^{(p)}| + \text{tr}[\mathbf{Q}_c^{(p)-1} \mathbf{Q}_c^{(q)}] + \|f_p(\mathbf{x}_0) - f_q(\mathbf{x}_0)\|_{\mathbf{Q}_c^{(p)-1}}^2, \quad (97) \end{aligned}$$

Now, taking the expectation under  $q(\mathbf{x}_0)$ , we have

$$\mathbb{E}_{q(\mathbf{x}_1, \mathbf{x}_0)} \log p(\mathbf{x}_1 | \mathbf{x}_0) = \log |2\pi \mathbf{Q}_c^{(p)}| + \text{tr}[\mathbf{Q}_c^{(p)-1} \mathbf{Q}_c^{(q)}] + \mathbb{E}_{q(\mathbf{x}_0)} \|f_p(\mathbf{x}_0) - f_q(\mathbf{x}_0)\|_{\mathbf{Q}_c^{(p)-1}}^2. \quad (98)$$

Thus, we have the following expression for the KL

$$D_{\text{KL}} [q(\mathbf{x}_1 | \mathbf{x}_0) \| p(\mathbf{x}_1 | \mathbf{x}_0)] = C(\mathbf{Q}_c^{(q)}, \mathbf{Q}_c^{(p)}) + \frac{1}{2} \mathbb{E}_{q(\mathbf{x}_0)} \|f_p(\mathbf{x}_0) - f_q(\mathbf{x}_0)\|_{\mathbf{Q}_c^{(p)-1}}^2, \quad (99)$$

where

$$C(\mathbf{Q}_c^{(q)}, \mathbf{Q}_c^{(p)}) = \frac{1}{2} \left( -\log \frac{|\mathbf{Q}_c^{(q)}|}{|\mathbf{Q}_c^{(p)}|} - d + \text{tr}[\mathbf{Q}_c^{(p)-1} \mathbf{Q}_c^{(q)}] \right). \quad (100)$$

When the two SSMs share the same transition noise,  $C(\mathbf{Q}_c^{(q)}, \mathbf{Q}_c^{(p)}) = 0$ .

## F CVI-DP method details

In this section we discuss the details about the proposed method CVI-DP. In App. F.1, we discuss the structure of the optimal posterior for the DP model. Then, in App. F.2, we exploit this structure and derive the update rules for CVI-DP.

### F.1 Structure of the optimal posterior

The ELBO in Eq. (18) can be understood as inference in the following generative model: the Gaussian process prior  $b$ , the observations  $\mathcal{D}$  and an additional likelihood whose expected logarithm is given by  $e(q, p, b)$ . For such a generative model, extending the results of [32, 12] to the continuous setting, the optimal variational Gaussian process  $q^*$  can be shown to have the following structure :

$$q^*(\mathbf{x}) \propto b(\mathbf{x}) \exp \left( \langle \phi_c(\boldsymbol{\lambda}^*) + \boldsymbol{\Lambda}^*, \mathbb{T}(\mathbf{x}) \rangle \right) \quad (101)$$

where  $\boldsymbol{\lambda}^*$  are sparse in time and depends on observations whereas  $\boldsymbol{\Lambda}^*$  are dense. They are defined via the self-consistency equations

$$\boldsymbol{\lambda}^* = \phi_c^{-1}(\nabla_{\boldsymbol{\mu}} \mathbb{E}_{q^*} \log p(\mathbf{y} | \mathbf{x})), \quad (102)$$

$$\boldsymbol{\Lambda}^* = \nabla_{\boldsymbol{\mu}} \mathbb{E}_{q^*} e(q[\boldsymbol{\mu}], p, b), \quad (103)$$

and the vector  $\mathbb{T}(\mathbf{x}) = (\mathbf{x}_t, \mathbf{x}_t(\mathbf{x}_t + d\mathbf{x}_t)^\top)$  is the sufficient statistics of a Gaussian distribution and  $\boldsymbol{\mu}(t) = \mathbb{E}_q[\mathbb{T}(\mathbf{x}_t)]$  are the expectation parameters that can be efficiently computed via smoothing.  $\boldsymbol{\lambda}$  and  $\boldsymbol{\Lambda}$  are often referred to as sites in the context of the expectation propagation algorithm.

The self-consistency equations of the optimal variational process can be obtained via the first order optimality condition as in Eq. (15).

In CVI-DP, we parameterize the natural parameters of the variational process as

$$\boldsymbol{\eta}_q = \boldsymbol{\eta}_b + \phi_c(\boldsymbol{\lambda}) + \boldsymbol{\Lambda}, \quad (104)$$

where  $\boldsymbol{\eta}_q$  and  $\boldsymbol{\eta}_b$  are the natural parameters of process  $q$  and  $b$  respectively.

### F.2 Derivation of the CVI-DP update rule

Starting from the ELBO in Eq. (18):

$$\mathcal{L}(q) = \mathbb{E}_q [\log p(\mathbf{y} | \mathbf{x})] + \underbrace{(D_{\text{KL}} [q \| b] - D_{\text{KL}} [q \| p])}_{e(q, p, b)} - D_{\text{KL}} [q \| b], \quad (105)$$

we parameterize the variational posterior  $q$  via its natural parameters as  $\boldsymbol{\eta}_q = \boldsymbol{\eta}_b + \phi_c(\boldsymbol{\lambda}) + \boldsymbol{\Lambda}$ . The mirror descent objective with step-size  $\rho$  is

$$\boldsymbol{\mu}^{(k+1)} = \arg \max_{\boldsymbol{\mu}} \langle \nabla_{\boldsymbol{\mu}} \mathcal{L}(\boldsymbol{\mu}) |_{\boldsymbol{\mu}^{(k)}}, \boldsymbol{\mu} \rangle - \frac{1}{\rho} D_{\text{KL}} [q(\mathbf{x}; \boldsymbol{\mu}) \| q(\mathbf{x}; \boldsymbol{\mu}^{(k)})]. \quad (106)$$

The gradient of the ELBO with respect to the expectation parameter can be written as

$$\nabla_{\boldsymbol{\mu}} \mathcal{L}(\boldsymbol{\mu})|_{\boldsymbol{\mu}^{(k)}} = \nabla_{\boldsymbol{\mu}} \mathbb{E}_q [\log p(\mathbf{y} | \mathbf{x})] |_{\boldsymbol{\mu}^{(k)}} + \nabla_{\boldsymbol{\mu}} e(q, p, b) |_{\boldsymbol{\mu}^{(k)}} - (\phi_c(\boldsymbol{\lambda}^{(k)}) + \boldsymbol{\Lambda}^{(k)}), \quad (107)$$

where we have used the property  $\nabla_{\boldsymbol{\mu}} \text{D}_{\text{KL}} [q \| b] = \boldsymbol{\eta}_q - \boldsymbol{\eta}_b = \phi_c(\boldsymbol{\lambda}) + \boldsymbol{\Lambda}$ .

To solution of the convex inner-maximization problem can be obtained by solving the first order optimality conditions

$$\boldsymbol{\eta}_q - \boldsymbol{\eta}_q^{(k)} = \rho \nabla_{\boldsymbol{\mu}} \mathcal{L}(\boldsymbol{\mu}) |_{\boldsymbol{\mu}^{(k)}}, \quad (108)$$

$$\implies \phi_c(\boldsymbol{\lambda}) + \boldsymbol{\Lambda} = \rho \nabla_{\boldsymbol{\mu}} \mathbb{E}_q [\log p(\mathbf{y} | \mathbf{x})] |_{\boldsymbol{\mu}^{(k)}} + \rho \nabla_{\boldsymbol{\mu}} e(q, p, b) |_{\boldsymbol{\mu}^{(k)}} + (1 - \rho)(\phi_c(\boldsymbol{\lambda}^{(k)}) + \boldsymbol{\Lambda}^{(k)}). \quad (109)$$

We distribute the two gradient terms to get the updates

$$\boldsymbol{\lambda}^{(k+1)} = (1 - \rho) \boldsymbol{\lambda}^{(k)} + \rho \phi_c^{-1} (\nabla_{\boldsymbol{\mu}} \mathbb{E}_q [\log p(\mathbf{y} | \mathbf{x})] |_{\boldsymbol{\mu}^{(k)}}), \quad (110)$$

$$\boldsymbol{\Lambda}^{(k+1)} = (1 - \rho) \boldsymbol{\Lambda}^{(k)} + \rho \nabla_{\boldsymbol{\mu}} e(q, p, b) |_{\boldsymbol{\mu}^{(k)}}. \quad (111)$$

The update rule for  $\boldsymbol{\Lambda}$  can be further simplified by using the property

$$\nabla_{\boldsymbol{\mu}} e(q, p, b) |_{\boldsymbol{\mu}^{(k)}} = \nabla_{\boldsymbol{\mu}} (\text{D}_{\text{KL}} [q \| b] - \text{D}_{\text{KL}} [q \| p]) |_{\boldsymbol{\mu}^{(k)}} \quad (112)$$

$$= \phi_c(\boldsymbol{\lambda}^{(k)}) + \boldsymbol{\Lambda}^{(k)} - \nabla_{\boldsymbol{\mu}} \text{D}_{\text{KL}} [q \| p] |_{\boldsymbol{\mu}^{(k)}}. \quad (113)$$

Therefore, the update can be equivalently written as

$$\boldsymbol{\Lambda}^{(k+1)} = \boldsymbol{\Lambda}^{(k)} + \rho (\phi_c(\boldsymbol{\lambda}^{(k)}) - \nabla_{\boldsymbol{\mu}} \text{D}_{\text{KL}} [q \| p] |_{\boldsymbol{\mu}^{(k)}}). \quad (114)$$

### F.3 Learning of model parameters

We denote the sum of the site contributions to the variational posterior by  $\Lambda = \phi_c(\boldsymbol{\lambda}) + \boldsymbol{\Lambda}$ . For the learning of the DP parameters  $\theta$ , the ELBO provides an objective which can be used as a proxy to the marginal likelihood:  $\ell(\theta) = \mathcal{L}(\boldsymbol{\eta}_q^*(\theta), \theta)$ . In practice, it is possible to obtain  $\boldsymbol{\eta}^*(\theta_0)$  for a given  $\theta_0$ , but the function  $\boldsymbol{\eta}^*(\theta)$  is intractable and therefore coordinate ascent is performed on  $\mathcal{L}(\boldsymbol{\eta}_q, \theta)$ . As discussed in Adam et al. [2], in the GP prior and Gaussian observation case, it is provably better to perform coordinate ascent in the  $(\Lambda, \theta)$  coordinates on the function  $l(\Lambda, \theta) = \mathcal{L}(\boldsymbol{\eta}_b(\theta) + \Lambda^*, \theta)$ , as opposed to coordinates ascent in  $(\boldsymbol{\eta}_q, \theta)$  on function  $\mathcal{L}(\boldsymbol{\eta}, \theta)$ . In this setting, we recover the marginal likelihood  $\log p(\mathbf{y}) = \mathcal{L}(\boldsymbol{\eta}_b(\theta) + \Lambda^*, \theta) > \mathcal{L}(\boldsymbol{\eta}_q^*(\theta_0), \theta)$ ,  $\forall \theta_0$ . In practice, this advantage further extends to more challenging observation models.

The objective we use for learning can be expressed as:

$$\begin{aligned} \mathcal{L}(\underbrace{\boldsymbol{\eta}_b(\boldsymbol{\theta}) + \Lambda^*}_{\boldsymbol{\eta}(\boldsymbol{\theta})}, \boldsymbol{\theta}) &= \mathbb{E}_{q_{\boldsymbol{\eta}(\boldsymbol{\theta})}(\mathbf{x})} \left[ \log \frac{\prod_{i=1}^n p(y_i | \mathbf{x}_i) p_{\boldsymbol{\theta}}(\mathbf{x})}{\frac{1}{\mathcal{Z}(\boldsymbol{\theta})} \prod_{i=1}^n t_i^*(\mathbf{x}_i) b_{\boldsymbol{\theta}}(\mathbf{x})} \right] \\ &= \log \mathcal{Z}_t(\boldsymbol{\theta}) + \underbrace{\mathbb{E}_{q_{\boldsymbol{\eta}(\boldsymbol{\theta})}(\mathbf{x})} \left[ \log \frac{p_{\boldsymbol{\theta}}(\mathbf{x})}{b_{\boldsymbol{\theta}}(\mathbf{x})} \right]}_{w(\boldsymbol{\theta})} + \underbrace{\sum_{i=1}^n \mathbb{E}_{q_{\boldsymbol{\eta}(\boldsymbol{\theta})}(\mathbf{x})} \left[ \log \frac{p(y_i | \mathbf{x}_i)}{t_i^*(\mathbf{x}_i)} \right]}_{c(\boldsymbol{\theta})}, \quad (115) \end{aligned}$$

where  $\log \mathcal{Z}_t(\boldsymbol{\theta})$  is the log-partition of  $\prod_{i=1}^n t_i^*(\mathbf{x}_i) b_{\boldsymbol{\theta}}(\mathbf{x})$ . It is the log marginal likelihood of a generative model where the prior is the linear DP,  $b_{\boldsymbol{\theta}}(\mathbf{x})$ , and the observation likelihoods are given by the Gaussian sites. Hence, this is classic Gaussian process regression. The term  $c(\boldsymbol{\theta})$  captures a notion of mismatch between the true likelihood terms and their Gaussian approximation via sites which is 0 in the setting of Gaussian observation model. The term  $w(\boldsymbol{\theta})$  is related to the error introduced by the linearization of the non-linear drift of the prior. This error is 0 when the prior is a linear DP.

## G Monte Carlo baselines

In the main paper, we compare to baseline ‘ground-truth’ solutions both for inferring the latent processes and for parameter learning targets. For inference, the problem falls under sequential Monte Carlo (particle smoothing) methods, and for estimating the approximate marginal likelihood we employ annealed importance sampling (AIS). In practice, we could use any simulation methods for the baseline, but we settle for the following setup due to its robustness and fast execution.

## G.1 Sequential Monte Carlo (SMC) baseline

We use a sequential Monte Carlo approach in the form of particle smoothing through conditional particle filtering with ancestor sampling. The posterior (smoothing) distribution  $p(\mathbf{x} | \mathbf{y})$  problem can not be computed in closed form in the general case due to the nonlinear nature of the models. We employ the approach of Svensson et al. [55], where the smoothing distribution  $p(\mathbf{x} | \mathbf{y})$  is approximated by generating  $K$  (correlated) samples using sequential Monte Carlo. Each iteration of the MCMC algorithm uses a conditional particle filter with ancestor sampling. This approach has been shown to avoid the problem of particle degeneracy typically occurring in particle filters [55].

As our setting is continuous-discrete (continuous-time prior with observations discretely spread over the time-horizon), we choose to use an Euler–Maruyama scheme with time-step size  $\Delta t$  for solving the SDE prior for discrete-time steps.

## G.2 Annealed importance sampling (AIS)

As an illustrative ground-truth for the parameter learning target (marginal likelihood), we use a sampling approach as the baseline. We use annealed importance sampling (AIS, [42]) which is similar to that used for Gaussian processes with non-conjugate likelihoods in Kuss and Rasmussen [35] and Nickisch and Rasmussen [44]. The setup defines a sequence of  $j = 0, 1, \dots, J$  steps  $Z_j = \int p(\mathbf{y} | \mathbf{x}; \theta)^{\tau(j)} p(\mathbf{x}; \theta) d\mathbf{x}$ , where  $\tau(j) = (j/J)^4$  (such that  $\tau(0) = 0$  and  $\tau(J) = 1$ ). The marginal likelihood can be rewritten as

$$p(\mathbf{y}; \theta) = \frac{Z_J}{Z_0} = \frac{Z_J}{Z_{J-1}} \frac{Z_{J-1}}{Z_{J-2}} \dots \frac{Z_1}{Z_0}, \quad (116)$$

where  $Z_j/Z_{j-1}$  is approximated by importance sampling using samples from  $q_j(\mathbf{x}) \propto p(\mathbf{y} | \mathbf{x}; \theta)^{\tau(j-1)} p(\mathbf{x}; \theta)$ :

$$\frac{Z_j}{Z_{j-1}} = \frac{\int p(\mathbf{y} | \mathbf{x}; \theta)^{\tau(j)} p(\mathbf{x}; \theta) d\mathbf{x}}{Z_{j-1}} \quad (117)$$

$$= \int \frac{p(\mathbf{y} | \mathbf{x}; \theta)^{\tau(j)} p(\mathbf{y} | \mathbf{x}; \theta)^{\tau(j-1)} p(\mathbf{x}; \theta)}{p(\mathbf{y} | \mathbf{x}; \theta)^{\tau(j-1)} Z_{j-1}} d\mathbf{x} \quad (118)$$

$$\approx \frac{1}{S} \sum_{s=1}^S p(\mathbf{y} | \mathbf{x}_j^{(s)}; \theta)^{\tau(j)-\tau(j-1)}, \quad \text{where } \mathbf{x}_j^{(s)} \sim \frac{p(\mathbf{y} | \mathbf{x}; \theta)^{\tau(j-1)} p(\mathbf{x}; \theta)}{Z_{j-1}}. \quad (119)$$

The difference to Kuss and Rasmussen [35] and Nickisch and Rasmussen [44] is that here sampling  $\mathbf{x}_j$  from  $p(\mathbf{y} | \mathbf{x}; \theta)^{\tau(j-1)} p(\mathbf{x}; \theta)/Z_{j-1}$  is non-trivial due to the non-linear/non-Gaussian nature of the prior. Here we use sequential Monte Carlo in the form of particle smoothing through conditional particle filtering with ancestor sampling (*i.e.*, the method presented in App. G.1) to draw those samples. For each process  $\mathbf{x}_j$  sampled from the SMC approach we only use the 10<sup>th</sup> sample (discarding the preceding ones as burn-in) and otherwise follow the setup described in App. G.1.

By using a single sample  $S = 1$  and a large number of steps  $J$ , the estimation of the log marginal likelihood can be written as

$$\log p(\mathbf{y}; \theta) = \sum_{j=1}^J \log \frac{Z_j}{Z_{j-1}} \approx \sum_{j=1}^J (\tau(j) - \tau(j-1)) \log p(\mathbf{y} | \mathbf{x}_j; \theta). \quad (120)$$

Following Kuss and Rasmussen [35], we set  $J = 8000$  and combine three estimates of log marginal likelihood by their geometric mean.

## H Details on experiments

In this section, we provide details for the experiments which were included in Sec. 4. We start by explaining the setup and details about the synthetic tasks (Sec. 4.1) for each diffusion process individually in App. H.1. We then cover the details about the experiments on real-world finance data and vehicle tracking (Sec. 4.2) in App. H.2 and App. H.3. We perform a grid search in all the experiments to find the best learning rate and other hyperparameters for all the methods.

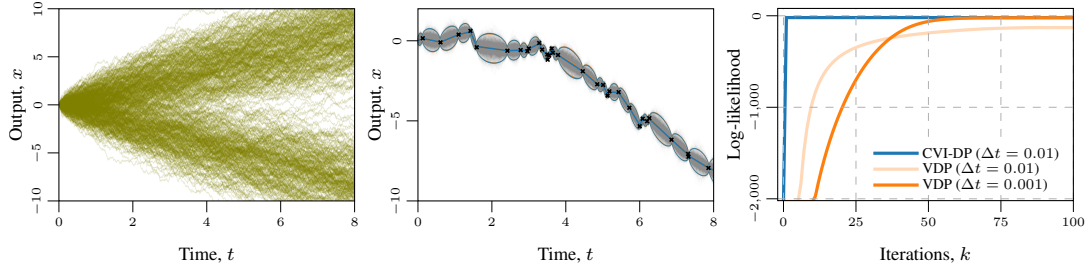


Figure 7: Approximate inference under a Beneš prior (draws from prior on the left). Middle: Approximate posterior processes for CVI-DP and VDP overlaid on the SMC ground-truth samples. Right: CVI-DP converges quickly even with large discretization step when inferring the variational parameters, while VDP suffers from slow convergence even with a small discretization step.

## H.1 Synthetic tasks: Inference and learning

We consider five diffusion processes to compare the performance of CVI-DP and VDP. For both inference and learning, 5-fold cross-validation is performed. We discuss each diffusion process and the experimental setup in detail below.

**Ornstein–Uhlenbeck** We start with the (linear) Ornstein–Uhlenbeck diffusion process as a sanity check where the exact posterior and the exact log-likelihood are available in closed-form. It is defined as

$$dx_t = -\theta x_t dt + d\beta_t, \quad (121)$$

where  $\beta_t$  is standard Brownian motion ( $Q_c = 1$ ). For the experiment, we set  $\theta = 0.5$ ,  $x_0 = 1$ ,  $t_0 = 0$ ,  $t_1 = 10$  and randomly observe 40 observations under the Gaussian likelihood with  $\sigma^2 = 0.01$ . To simulate the process, Euler–Maruyama is used with 0.01 step-size.

For inference, both the methods (CVI-DP and VDP) have an Ornstein–Uhlenbeck DP as prior with  $\theta = 1.2$  and  $Q_c = 1.0$ . To get the (exact) posterior and the (exact) log-marginal likelihood, we use a Gaussian process regression (GPR) model with a matched Matérn- $1/2$  kernel. In the linear DP setup, CVI-DP does a single-step update with  $\rho = 1$  for all values of the discretization grid ( $\Delta t = \{0.01, 0.005, 0.001\}$ ) (theoretical reason of the single-step update is discussed in Sec. 3.2). For VDP, we perform a grid-search over various learning-rate  $\omega$  and use the best-performing one: 1.0 for  $\Delta t = 0.001$ , 0.5 for  $\Delta t = 0.005$ , and 0.1 for  $\Delta t = 0.01$ . As all the models converge to the same posterior, the posterior obtained by CVI-DP with  $\Delta t = 0.01$  is only plotted in Fig. 3 along with the convergence plot for all the methods.

For learning, the same setup as in the inference experiment is used, but the parameter  $\theta$  of the prior OU (lengthscale and variance of Matérn- $1/2$  kernel in GPR) is also optimized. For all the methods,  $\theta$  is initialized to 2.5 (to be off from the expected optima) and the Adam optimizer is used. For the learning rate of Adam optimizer, we perform a grid search and use the best-performing one: 0.1 for CVI-DP and 0.01 for VDP.

**Beneš** We experiment with a commonly used non-linear diffusion process, the Beneš DP, whose marginal state distributions are bimodal and mode-switching in sample state trajectories becomes increasingly unlikely with time (Fig. 7). It is defined as:

$$dx_t = \theta \tanh(x_t) dt + d\beta_t, \quad (122)$$

where  $\beta_t$  is standard Brownian motion ( $Q_c = 1$ ). For the experiment, we set  $\theta = 1.0$ ,  $x_0 = 0$ ,  $t_0 = 0$ ,  $t_1 = 8$  and randomly observe 40 observations under the Gaussian likelihood with  $\sigma^2 = 0.01$ . To simulate the process, Euler–Maruyama is used with 0.01 step-size.

For inference, both the methods (CVI-DP and VDP) have a Beneš DP as prior with  $\theta = 1.0$  and  $Q_c = 1.0$ . After performing a grid search over the learning rate for both the methods, we use the best performing one:  $\rho = 1$  in CVI-DP for all discretization grid ( $\Delta t = \{0.01, 0.005, 0.001\}$ ), and  $\omega = 0.1$  for  $\Delta t = 0.001$ ,  $\omega = 0.001$  for  $\Delta t = \{0.005, 0.01\}$  for VDP. The posterior of both methods and the convergence plot are shown in Fig. 7. From the plot, it can be observed that the posterior obtained by both methods is identical. However, CVI-DP converges faster than VDP.

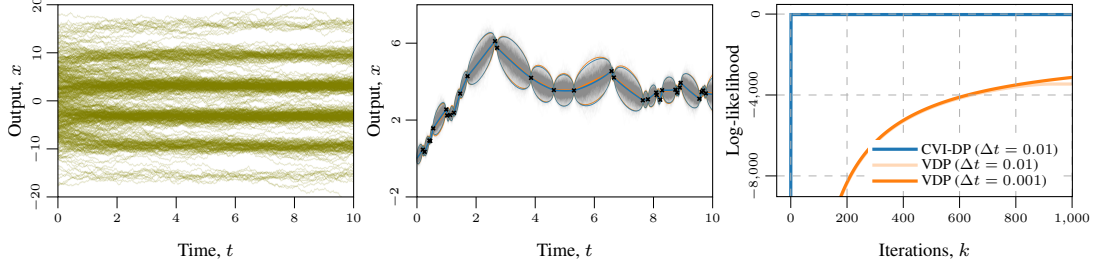


Figure 8: Approximate inference under a Sine prior (draws from prior on the left). Middle: Approximate posterior processes for CVI-DP and VDP overlaid on the SMC ground-truth samples. Right: CVI-DP converges quickly even with large discretization step when inferring the variational parameters, while VDP suffers from slow convergence even with a small discretization step.

For learning, the same setup as in the inference experiment is used, and now the parameter  $\theta$  of the prior Beneš DP is also optimized. For both methods,  $\theta$  is initialized to 3 (to be off from the expected optima), and Adam optimizer is used. For the learning rate of Adam optimizer, we perform a grid search and use the best-performing one: 0.1 for CVI-DP and 0.01 for VDP.

**Double-well** We experiment with the non-linear diffusion process, the double-well (DW) DP, whose marginal state distributions have two modes that sample state trajectories keep visiting through time (Fig. 4). It is defined as:

$$dx_t = \theta_0 x_t (\theta_1 - x_t^2) dt + d\beta_t, \quad (123)$$

where  $\beta_t$  is standard Brownian motion ( $Q_c = 1$ ). For the experiment, we set  $\theta_0 = 4.0$ ,  $\theta_1 = 1.0$ ,  $x_0 = 1.0$ ,  $t_0 = 0$ ,  $t_1 = 20$  and randomly observe 40 observations under the Gaussian likelihood with  $\sigma^2 = 0.01$ . To simulate the process, Euler–Maruyama is used with 0.01 step-size.

For inference, both the methods (CVI-DP and VDP) have a double-well DP as prior with  $\theta_0 = 4.0$ ,  $\theta_1 = 1.0$  and  $Q_c = 1.0$ . After performing a grid search over the learning rate for both the methods, we use the best performing one:  $\rho = 0.5$  for CVI-DP and  $\omega = 0.001$  for VDP for all discretization grid ( $\Delta t = \{0.01, 0.005, 0.001\}$ ). The posterior of both methods and the convergence plot are shown in Fig. 4. The plot shows that VDP struggles with convergence issues while CVI-DP converges faster and to a better ELBO value. With optimization tricks and more iterations, VDP is expected to reach the same posterior as CVI-DP.

For learning, the same setup as in the inference experiment is used, and now the parameter  $\theta_1$  of the prior DW DP is also optimized. For both the methods,  $\theta_1$  is initialized to 0.0 (to be off from the expected optima), and Adam optimizer is used. For the learning rate of Adam optimizer, we perform a grid search and use the best-performing one: 0.1 for CVI-DP and 0.01 for VDP. Fig. 5 showcases the fast learning of  $\theta_1$  in CVI-DP as compared to VDP.

**Sine** We experiment with the non-linear diffusion process, Sine DP, whose marginal state distributions have many modes (Fig. 8). It is defined as:

$$dx_t = \theta_0 \sin(x_t - \theta_1) dt + d\beta_t, \quad (124)$$

where  $\beta_t$  is standard Brownian motion ( $Q_c = 1$ ). For the experiment, we set  $\theta_0 = 1.0$ ,  $\theta_1 = 0.0$ ,  $x_0 = 0$ ,  $t_0 = 0$ ,  $t_1 = 10$  and randomly observe 40 observations under the Gaussian likelihood with  $\sigma^2 = 0.01$ . To simulate the process, Euler–Maruyama is used with 0.01 step-size.

For inference, both the models (CVI-DP and VDP) have a Sine DP as prior with  $\theta_0 = 1.0$ ,  $\theta_1 = 0.0$ , and  $Q_c = 1.0$ . After performing a grid search over the learning rate for both the methods, we use the best performing one:  $\rho = 1.0$  for CVI-DP and  $\omega = 10^{-5}$  for VDP for all discretization grid ( $\Delta t = \{0.01, 0.005, 0.001\}$ ). The posterior and convergence plot of both methods is shown in Fig. 8. From the plot, it can be observed that the posterior obtained by both methods is identical. However, CVI-DP converges faster than VDP. For VDP, in the experiment, we set the maximum iterations to 1000. However, with more iterations and optimization tricks, VDP is expected to reach the same ELBO value as CVI-DP. Empirically, we found that VDP suffers from slow convergence and takes  $\sim 7000$  iterations to lead to a value closer to CVI-DP.

For learning, the same setup as in the inference experiment is used, and now the parameter  $\theta_1$  of the prior Sine DP is also optimized. For both methods,  $\theta_1$  is initialized to 2.0 (to be off from the

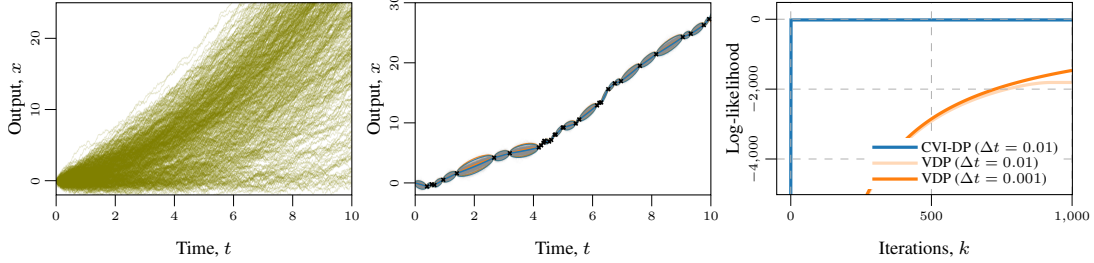


Figure 9: Approximate inference under a Sqrt prior (draws from prior on the left). Middle: Approximate posterior processes for CVI-DP and VDP overlaid on the SMC ground-truth samples. Right: CVI-DP converges quickly even with large discretization step when inferring the variational parameters, while VDP suffers from slow convergence even with a small discretization step.

expected optima), and Adam optimizer is used. For the learning rate of Adam optimizer, we perform a grid search and use the best-performing one: 0.01 for both CVI-DP and VDP. While learning, after performing a grid search, the best-performing learning rate for CVI-DP was  $\rho = 0.1$  while for VDP, it was the same as in inference,  $\omega = 10^{-5}$ .

**Square-root** We experiment with the non-linear diffusion process, Square-root DP, that has divergent fat-tailed behaviour (Fig. 9). It is defined as:

$$dx_t = \sqrt{\theta|x_t|} dt + d\beta_t, \quad (125)$$

where  $\beta_t$  is the standard Brownian motion ( $Q_c = 1$ ). For the experiment, we set  $\theta = 1.0$ ,  $x_0 = 0.0$ ,  $t_0 = 0$ ,  $t_1 = 10$  and randomly observe 40 observations under the Gaussian likelihood with  $\sigma^2 = 0.01$ . To simulate the process, Euler–Maruyama is used with 0.01 step-size.

For inference, both the models (CVI-DP and VDP) have a Square-root DP as prior with  $\theta = 1.0$  and  $Q_c = 1.0$ . After performing a grid search over the learning rate for both the methods, we use the best performing one:  $\rho = 1.0$  for CVI-DP and  $\omega = 10^{-5}$  for VDP for all discretization grid ( $\Delta t = \{0.01, 0.005, 0.001\}$ ). The posterior and convergence plot of both methods is shown in Fig. 8. From the plot, it can be observed that the posterior obtained by both methods is identical. However, CVI-DP converges faster than VDP. For VDP, in the experiment, we set the maximum iterations to 1000. However, with more iterations and optimization tricks, VDP is expected to reach the same ELBO value as CVI-DP. Empirically, we found that VDP suffers from slow convergence and takes  $\sim 7000$  iterations to lead to a value closer to CVI-DP.

For learning, the same setup as in the inference experiment is used, and now the parameter  $\theta$  of the prior Sine DP is also optimized. For both methods,  $\theta$  is initialized to 5.0 (to be off from the expected optima), and Adam optimizer is used. For the learning rate of Adam optimizer, we perform a grid search and use the best-performing one: 0.01 for both CVI-DP and VDP. While learning, after performing a grid search, the best-performing learning rate for CVI-DP was  $\rho = 0.5$  while for VDP, it was the same as in inference,  $\omega = 10^{-5}$ .

## H.2 Finance data

While the main focus is on providing a better method and algorithm for the particular case defined by VDP (and thus benchmark primarily against it), we also seek to showcase the practical applicability of our approach. To showcase the capability of proposed method CVI-DP in the real world, we experiment with a finance data set originally proposed for Student- $t$  processes in [53]. The data set considers the (log) stock price of Apple Inc. and consists of 8537 trading days (setup follows [53]). This experiment aims to learn the underlying process of the stock price, which is measured in terms of negative log predictive density (NLPD) on the hold-out test set. We bin the data into five bins,  $\sim 1707$  trading days in every bin and model the log stock price. We experiment with three models; each model has different prior information incorporated in it. Gaussian likelihood is used with  $\sigma^2 = 0.25$  for all the models, which is not optimized.

Following Solin and Särkkä [53], we consider a GP baseline: sparse variational Gaussian process (SVGP) with 500 inducing points [57] in which prior information is incorporated in terms of the

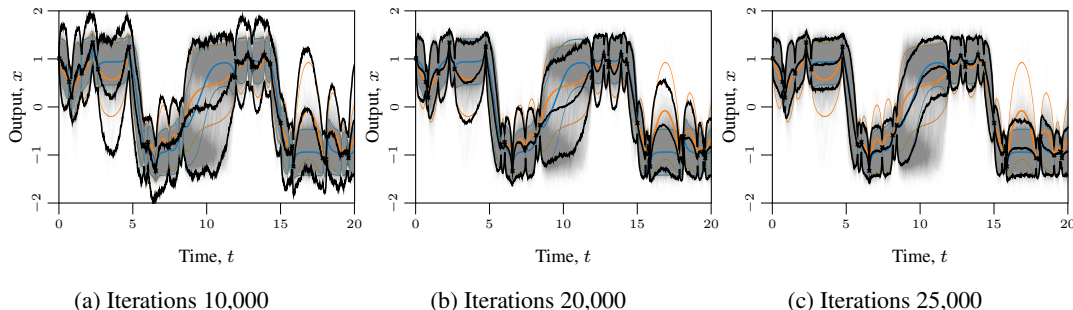


Figure 10: Approximate posterior processes under a Double-Well prior (setup similar to Fig. 4) for — CVI-DP, — VDP, and — NeuralSDE [33] with different iterations overlaid on the SMC ground-truth samples. The NeuralSDE posterior gets closer to CVI-DP with more iterations.

sum of kernels (Const.+Lin.+Matérn- $3/2$ +Matérn- $1/2$ ). The prior is structured as in [53] to capture a linear trend, a slowly moving smooth trend component, and a faster more volatile component. The GP baseline gives NLPD  $1.44 \pm 0.70$  / RMSE  $0.91 \pm 0.54$ . All the kernels are initialized with unit variance and lengthscale, and Adam optimizer is used with a learning rate of 0.1. The inducing variables are spread uniformly over the time grid and not optimized.

Next, we experiment with CVI-DP with a linear OU DP process in which prior is incorporated in terms of the OU process, which is initialized with  $\theta=1.0$ ,  $Q_c=0.1$ . After evaluating the data, the prior on the initial state is set to  $N(-1, 0.1)$ . The learning rate  $\rho$  is set to 1.0 and the prior DP parameter is optimized using Adam optimizer with a 0.01 learning rate. The model gives NLPD  $1.08 \pm 0.45$  / RMSE  $0.77 \pm 0.41$ .

Finally, to give more flexibility, we experiment with CVI-DP with a neural network drift (NN) DP. The drift of the prior DP  $f_p$  is initialized to be a NN with one hidden layer with three nodes followed by a ReLU activation function, and  $Q_c$  is set to 0.1. The parameters of the NN are initialized from a unit Gaussian, and after evaluating the data, prior on the initial state is set to  $N(-1, 0.1)$ . The learning rate  $\rho$  is set to 0.5 and the prior DP parameter is optimized using Adam optimizer with  $10^{-3}$ . The model gives NLPD  $0.81 \pm 0.08$  / RMSE  $0.51 \pm 0.08$ .

Of all the models, CVI-DP with a NN as drift results in the best NLPD / RMSE value as it is the most flexible and can adapt to the non-stationary behaviour of the data over the state range. To show the quality of learnt drift, we simulate and plot the predictions from the learnt prior DP for future years Fig. 6.

### H.3 GPS tracking data

To further showcase the applicability of CVI-DP in real-world, we experiment with a GPS data set of a moving vehicle (data also from [53]). The aim is to model the 2D trajectory of the vehicle recorded from GPS coordinates over time. The data set is 106 minutes long and consists of 6373 observation points. We experiment with two models; both use two independent DPs learnt jointly (one for latitude and one for longitude directions). Similar to the setup in [53], we split the data in chunks of 30 s and perform 10-fold cross-validation. For all the models, Gaussian likelihood is used with  $\sigma^2 = 0.01$ , which is not optimized.

First, we experiment with CVI-DP with a linear OU DP process in which prior is incorporated in terms of the OU process, which is initialized with  $\theta = 1.0$ ,  $Q_c = 0.1$ . After evaluating the data, prior on the initial state is set to  $N(0, 0.1)$ . For optimizing sites, the learning rate  $\rho$  is set to 0.5, and the prior DP parameter  $\theta$  is optimized using Adam optimizer with a 0.01 learning rate. The model gives NLPD  $-0.67 \pm 0.19$  / RMSE  $0.13 \pm 0.04$ . Next, similar to the finance example (App. H.2), to give more flexibility, we experiment with CVI-DP with a neural network (NN) drift DP  $f_p$ . The drift of the DP is initialized

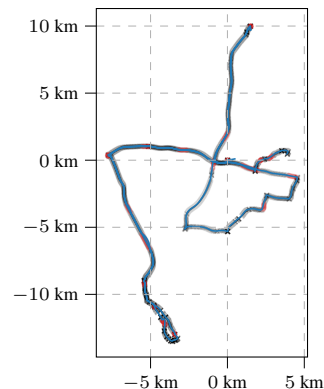


Figure 11: Approximate posterior process of CVI-DP with NN drift on GPS data along with the observations.

to be a NN with one hidden layer with three nodes followed by a ReLU activation function, and  $Q_c$  is set to 0.1. The parameters of the NN are initialized from a unit Gaussian, and after evaluating the data, prior on the initial state is set to  $N(0, 0.1)$ . The learning rate  $\rho$  is set to 0.5 and the prior DP parameter is optimized using Adam optimizer with  $10^{-2}$  learning rate. The model gives NLPD  $-0.82 \pm 0.43$  / RMSE  $0.06 \pm 0.03$ .

CVI-DP with a NN drift gives better NLPD and RMSE value primarily because of the flexibility of the DP to model the trajectory and possibility to adapt to the non-stationary behaviour in the state space. The posterior for CVI-DP with NN drift is shown in Fig. 11. The behaviour of the vehicle is different at different points in the input space (perhaps due to faster driving on highways and slower on smaller streets), which the model is able to capture by learning the parameters.

#### H.4 Comparison with NeuralSDEs

We also compare against the recently popular class of NeuralSDE methods [36, 33]. These methods are variational inference algorithms with a broader scope than CVI-DP: the posterior process  $q$  is not restricted to be a linear DP but is characterized by a neural network drift. However, they rely on sample-based simulation methods for estimation of the ELBO gradient and thus incur a large computational cost. Also, the convergence of optimization via stochastic gradient descent is often slow.

Empirically, we find that these methods need a delicate learning-rate scheduler to converge. In comparison, CVI-DP has a deterministic objective and intrinsically has an adaptive learning rate (setup similar to various natural gradient descent algorithms). Thus, CVI-DP is fast and does not need fine-tuning. Fig. 10 showcases the posterior of NeuralSDE along with CVI-DP and VDP (similar to Fig. 4). From the figure, it can be noted that in fewer iterations, the posterior is similar to VDP and with more iterations, the posterior gets closer to what CVI-DP gets. For the experiment, we use 1000 training samples for each iteration step and Adam optimizer with a 0.1 learning rate and an exponential learning-rate scheduler. The implementation is based on the code-base of Kidger et al. [33].

Fig. 10 shows that while the NeuralSDE approach is general and eventually converges to the same optima as CVI-DP, in the particular case where it is possible to formalize the problem under the VDP/CVI-DP setting, using CVI-DP for inference and learning is orders of magnitude faster.

## I Author contributions

The initial idea and motivation of this work was conceived by VA in discussion with PV. PV had the main responsibility of implementing the method and conducting the experiments with help from AS and VA. The first draft was written by VA and PV. All authors contributed to finalizing the manuscript.